

SEMMELWEIS EGYETEM
DOKTORI ISKOLA

Ph.D. értekezések

3464.

GÉM JANKA BORBÁLA

Celluláris és molekuláris élettan

című program

Programvezető: Dr. Hunyady László, egyetemi tanár

Témavezető: Dr. Hunyady László, egyetemi tanár

Dr. Balla András, egyetemi docens

Investigation of Angiotensin II-induced Gene Expression Changes In Vascular Smooth Muscle Cells

PhD thesis

Janka Borbála Gém, MD

Semmelweis University Doctoral School
Molecular Sciences Division



Supervisors: László Hunyady, MD, Ph.D, D.Sc
András Balla, Ph.D, D.Sc

Official reviewers: Fagyas Miklós, MD, Ph.D
Dézsi László, MD, Ph.D, Med. Habil.

Head of the Complex Examination Committee:
Szabolcs Várbíró, MD, Ph.D, Med. Habil.

Members of the Complex Examination Committee:
Éva Ruisanchez, MD, Ph.D
Anita Alexa, Ph.D

Budapest
2026

Table of Contents

List of Abbreviations.....	6
1. Introduction.....	9
1.1. Overview.....	9
1.2. The renin-angiotensin-aldosterone system	10
1.3. Effects of AngII on different cell types.....	11
1.4. Further elements and functions of the RAAS	12
1.5 The angiotensin type 1 receptor.....	14
1.5.1. The structure of AT1R	14
1.5.2. Activation of AT1R.....	15
1.5.3. Signal transduction of AT1R.....	16
1.5.3.1. G protein-dependent pathways	16
1.5.3.2. G protein-independent pathways	17
1.6. The MAPK cascade	18
1.7. Dual-specificity phosphatases	20
1.8. AngII mediated EGFR transactivation.....	22
1.8.1. The EGFR	23
1.8.2. Transactivation of EGFR by AT1R activation.....	23
1.9. LMCD1.....	23
2. Objectives.....	25
2.1. Aims related to AngII-mediated gene expression changes:.....	25
2.2. Aims related to EGFR transactivation:	25
3. Methods.....	26
3.1. Materials	26
3.2. Cell cultures.....	26
3.3. Plasmid constructs	27
3.3.1. LMCD1 Overexpressing plasmid constructs	27
3.3.2. <i>EGFR</i> silencing and lentivirus production	27
3.4. Affymetrix GeneChip Assay	28
3.5. Plasmid transfection.....	28
3.6. Lentiviral infection	29
3.7. Stimulation and pharmacological inhibitor treatments	29

3.8. Gene expression measurements	29
3.9. Immunostaining	30
3.10. Western blot assay	31
3.11. ³ H-Leucine incorporation assay	31
3.12. Wound-healing assay	32
3. 13. Statistical analysis.....	32
4. Results.....	33
4.1. Gene expression changes in VSMCs to AngII stimulation	33
4.1.1. Affymetrix gene-chip assay	33
4.2. AngII-mediated upregulation of <i>LMCD1</i> in VSMCs	34
4.2.1. Kinetic changes over time of <i>LMCD1</i> gene and protein expression in response to AngII.....	34
4.2.2. Intracellular localization of <i>LMCD1</i>	36
4.2.3. Role of AT1R and G-protein coupling in AngII mediated <i>LMCD1</i> expression.....	37
4.2.4. Role of secondary messengers in the upregulation of <i>LMCD1</i>	39
4.2.5. Role of MAPKs in AngII-mediated <i>LMCD1</i> upregulation	41
4.3. Investigation of functional role of <i>LMCD1</i> in vascular smooth muscle cells	43
4.3.1. Effect of <i>LMCD1</i> on cellular proliferation and migration	43
4.4. Importance of EGFR transactivation in AngII mediated gene expression changes.....	45
4.4.1. Identification of additional gene targets.....	45
4.4.2. Lentiviral silencing of <i>EGFR</i>	47
4.4.3. Comparing pharmacological inhibition and genetic silencing of EGFR	48
4.4.3.1. Effect of pharmacological inhibition of EGFR transactivation on AngII-mediated upregulation of <i>DUSP</i> isoforms	49
4.4.3.2. Effect of shRNA mediated silencing of <i>EGFR</i> on AngII-induced upregulation of <i>DUSP</i> isoforms	51
4.4.4. Potential pathways beside EGFR-transactivation	52
5. Discussion	54
6. Conclusions	59
7. Summary	53
8. References	54
9. Bibliography of candidate's publications.....	59
9.1. Publications relevant to the dissertation	59
9.2. Publications unrelated to the dissertation	59
10. Acknowledgements	61

List of Abbreviations

ACE	Angiotensin converting enzyme
ADAM	A disintegrin and metalloproteinase
Ang(1-7)	Angiotensin (1-7)
AngA	Angiotensin A
AngI	Angiotensin I
AngII	Angiotensin II
AngIII	Angiotensin III
AngIV	Angiotensin IV
APA	Aminopeptidase A
APN	Aminopeptidase N
AT1R	Angiotensin type 1 receptor
AT2R	Angiotensin type 2 receptor
AT4R	Angiotensin type 4 receptor
AVP	Arginine-vasopressin
BSA	Bovine serum albumin
CaMKII	Ca ²⁺ /calmodulin-dependent protein kinase II
CNS	Central nervous system
DAG	Diacylglycerol
DMEM	Dulbecco's modified eagle medium
DNA	Deoxyribonucleic acid
DPI	Diphenyleneiodonium chloride
DUSP	Dual-specificity phosphatase
EGF	Epithelial growth factor
EGFR	Epithelial growth factor receptor
ERK	Extracellular regulated kinase
FAK	Focal adhesion kinase
FBS	Fetal bovine serum
GAPDH	Glyceraldehyde-3-phosphate dehydrogenase
GATA	Glycine-Adenine-Thymine-Adenine

GFR	Glomerular filtration rate
GPCR	G protein coupled receptor
Hb-EGF	Heparin-binding EGF-like growth factor
IGFR	Insulin-like growth factor receptor
IP3	Inositol-3,4,5-trisphosphate
IP3R	Inositol-3,4,5-trisphosphate receptor
IRAP	Insulin regulated aminopeptidase
JAK	Janus kinase
JNK	Jun-kinase
KIM	Kinase interacting motif
LIM	Lin-11, Isl-1 and Mec-3
LMCD1	Lim and cysteine rich domain 1
MAPK	Mitogen activated protein kinase
Mas	Mas oncogene
MEK	Mitogen activated protein kinase kinase
MKB	MAP kinase binding domain
MMP	Matrix-metalloproteinase
MR	Mineralocorticoid receptor
Mrg D	Mas-related G protein coupled receptor D
mRNA	Messenger RNA
NOX	NADPH oxidase
PCR	Polymerase chain reaction
PDGFR	Platelet derived growth factor receptor
PET	Prickle, Espinas and Testin
PFA	Paraformaldehyde
PI3K	Phosphatidil-inositol 3 kinase
PKC	Protein kinase C
PLC	Phospholipase C
PMA	Phorbol myristate acetate
PTK	Protein tyrosine kinase
qPCR	Quantitative PCR
RAAS	Renin-angiotensin-aldosterone system

RISC	RNA-induced silencing complex
RNA	Ribonucleic acid
ROS	Reactive oxygen species
shRNA	Short hairpin RNA
STAT	Signal transducer and activator of transcription proteins
TCA	Trichloroacetic acid
VSMC	Vascular smooth muscle cell

1. Introduction

1.1. Overview

The aim of this thesis is to characterize the gene expression changes mediated by angiotensin II (AngII) and their long-term effects in vascular smooth muscle cells (VSMCs), with particular attention to the upregulation of LIM and cysteine-rich domains 1 (LMCD1) and the role of transactivation of the epidermal growth factor receptor (EGFR) by the angiotensin type 1 receptor (AT1R).

Exaggerated activation of AT1R in VSMCs is known to be a major factor in the pathogenesis of common and severe cardiovascular diseases such as hypertension and atherosclerosis. These pathological changes in the vasculature often lead to potentially fatal events such as stroke or myocardial infarction (1). AT1R is primarily activated by AngII, an octapeptide hormone that serves as the main effector of the renin-angiotensin-aldosterone system (RAAS), which plays a key role in regulating body fluid volume, sodium homeostasis, and systemic blood pressure (2). In clinical pharmacology, small-molecule inhibitors of angiotensin-converting enzyme (ACE) and AT1R are widely used and effective treatments for high blood pressure (3). On the one hand, AngII-mediated activation of AT1R causes immediate vasoconstriction of VSMCs, resulting in a rapid elevation of systemic blood pressure. On the other hand, AT1R activation also induces long-term effects—primarily through gene expression changes—that lead to structural remodeling of the vessel wall. This remodeling process involves proliferation, migration, and increased fibrosis of the tunica media, ultimately causing significant alterations in the hemodynamic properties of the vessels (2). A critical component of AngII-induced gene expression changes is the transactivation of various receptor tyrosine kinases, including EGFR. One of the key downstream effectors of growth factor receptors is the family of mitogen-activated protein kinases (MAPKs)—serine-threonine kinases well known for their proliferative effects (4).

Our research group conducted an Affymetrix gene chip assay on primary VSMCs to investigate their gene expression response to AngII stimulation. This approach identified a substantial number of genes significantly upregulated by AngII. In this thesis, I aim to focus on *LMCD1*, a gene found to be strongly upregulated in response to AngII.

I intend to explore the signaling pathways responsible for its upregulation and to characterize its functional effects on VSMCs. Additionally, I examine the EGFR transactivation by AT1R in the context of various dual-specificity phosphatase (DUSP) isoforms—namely DUSP5, DUSP6, and DUSP10—which were also found to be upregulated by AngII in VSMCs.

1.2. The renin-angiotensin-aldosterone system

The renin-angiotensin-aldosterone system (RAAS) is a key regulator of body fluid volumes, more specifically it is responsible for the regulation of water uptake, sodium (Na^+) homeostasis, and systemic blood pressure. The activation of the RAAS depends on the renin secretion from the juxtaglomerular cells of the kidney. Renin is stored in the granules of juxtaglomerular cells and released as an active enzyme. Renin secretion can be triggered through several mechanisms. First, the renin secretion can be initiated directly by mechanosensitive receptors that sense the arterial blood pressure decrease. Second, it can be stimulated indirectly in the distal tubules of the kidney by the cells of macula densa, which are highly sensitive to the Na^+ concentration of the tubular fluid. When the filtrated Na^+ level decreases, the cells of macula densa initiate renin release of the juxtaglomerular cells. Additionally, the sympathetic nervous system is also capable of increase the renin release via β 1-adrenergic receptor activation (5).

After its release into the blood plasma, renin functions as a protease. It cleaves the N-terminus of angiotensinogen, which is a liver-derived α 2-globuline. The produced decapeptide is called angiotensin I (AngI), also known as pro-angiotensin. AngI itself has no known biological effect, it serves as the precursor of AngII. in order to be converted to active AngII, it must interact with angiotensin-converting enzyme (ACE) (6). ACE is mainly found on the surface of endothelial cells, especially in the lungs, although its presence has also been detected on epithelial, nervous, and gonadal cells. ACE is a zinc metalloproteinase enzyme that hydrolyzes the C-terminus of AngI, converting it to the biologically active octapeptide hormone, AngII (6). In the human body, AngII exerts its effects through two different receptors, angiotensin type 1 receptor (AT1R) and angiotensin type 2 receptor (AT2R), both of are members of the G protein-coupled receptor (GPCR) family. Interestingly, AT1R and AT2R have very distinct and often opposing biological effects. While AT1R activation causes mainly hypertensive

responses, AT2R is associated mainly with antihypertensive effects (7). Furthermore, the ACE is able to degrade AngII into smaller, primarily antihypertensive peptides. Due to the activity of various peptidases, AngII has a short half-life in plasma, lasting only a few seconds before being converted into metabolites such as AngIII and Ang(1–7) (8,9).

1.3. Effects of AngII on different cell types

AngII has numerous effects on various cell types. In the cells of zona glomerulosa in the adrenal gland cortex, AngII stimulation initiates the release of aldosterone. Aldosterone is a steroid hormone that exerts its effects on an intracellular receptor, the mineralocorticoid receptor (MR). Although MR is expressed in several tissues, it exerts its most prominent effects in the epithelial cells of the renal collecting tubules. As an intracellular receptor, MR regulates gene expression changes in aldosterone's target cells. There, the activation of MR leads to increased Na⁺ reabsorption and K⁺ secretion, making aldosterone pivotal in salt and water homeostasis (10).

AngII also acts within the central nervous system. In the cells of area postrema and in the subfornical organ of the brain, AngII causes a dipsogenic effect, increasing the thirst drive to water uptake and also increases salt appetite (11). Furthermore, in the posterior part of the pituitary gland, AngII increases the arginine-vasopressin (AVP) release, which is another important hormone in salt and water homeostasis (12).

In the kidney, AngII has its own direct effects on the cells of the proximal tubules by increasing Na⁺ reabsorption. However, its most important effects on kidney function are exerted on the smooth muscle cells of the afferent and efferent arterioles, thereby regulating the glomerular filtration rate (GFR). By causing vasoconstriction in the efferent arterioles, AngII increases the hydrostatic pressure in the glomerular capillaries, leading to increased filtration and elevated GFR (13).

From the perspective of this PhD thesis, AngII exerts its most important effects in the cardiovascular system. In VSMCs, the activation of AT1R by AngII causes fast-emerging, short-term responses and slowly evolving, long-term effects on gene expression levels. The most important and most spectacular short-term effect of AngII in VSMCs is the rapid vasoconstriction by increasing the intracellular Ca²⁺ level, consequently elevating systemic blood pressure. One of the long-term effects are that AngII can initiate signaling pathways that lead to changes in gene expression. These

chronic effects mainly regulate cell proliferation, migration, extracellular matrix production, and cell survival and the main contributors to the development of pathological conditions such as hypertension and atherosclerosis (2). Both the short- and long-term effects of AngII hormone will be discussed in detail in subsequent chapters.

1.4. Further elements and functions of the RAAS

In recent decades, additional elements and functions of the RAAS have been discovered beyond the classical ones previously described.

Cleaving the N-terminal aspartate amino-acid of AngII, the glutamyl aminopeptidase A (APA) converts AngII to AngIII. AngIII can also induce vasoconstriction in VSMCs, but its pressor effect is much weaker compared to AngII. Interestingly, AngIII appears to be equally effective as AngII in the stimulation of aldosterone release from zona glomerulosa cells. Moreover, by interacting with AT2R, AngIII induces an even stronger natriuretic effect than AngII (9).

AngIII can be further cleaved by aminopeptidase N (APN) to produce hexapeptide AngIV, by removing its N-terminal arginine. AngIV seems to exert its effects mainly within the CNS. It has been shown that AngIV can bind as a ligand to insulin-regulated aminopeptidase (IRAP), also referred as angiotensin type 4 receptor (AT₄R), which is predominantly expressed in the hippocampus. Evidence suggests that AngIV may play a role in learning processes and memory (14).

AngII can also be converted by mononuclear leukocyte-derived aspartate decarboxylase to Angiotensin A (AngA), with its N-terminal Asp being changed to Ala. AngA exhibits similar affinity to AT₁R as AngII, but its affinity to AT₂R is significantly higher. AngA, similarly to AngII, is also a vasoconstrictive peptide, though it has lower vasoconstrictor potency than AngII (15).

Angiotensin converting enzyme 2 (ACE2) is predominantly expressed as a cell surface protein in the intestines, kidneys, gallbladder, testes, and heart. ACE2 is capable of cleaving both AngI and AngII to produce Ang(1-7). The Ang(1-7) has been proven to exert vasodilatory effects by interacting with Mas receptor, thus it mainly functions as a negative feedback mechanism of the RAAS. ACE2 can also convert AngA to alamandine by cleaving its C-terminal phenylalanine. Alamandine exerts its effects through Mas-related (Mas oncogene-related) G protein-coupled receptor D (MrgD

receptor) and has been described to have mainly antihypertensive and cardioprotective effects *in vivo*. Alamandine can also be converted from Ang(1-7) by decarboxylation on its N-terminal Asp (8,15). (Figure 1.) . Notably, ACE2 serves as an entry point for various coronaviruses including SARS-CoV and SARS-CoV-2 (16).

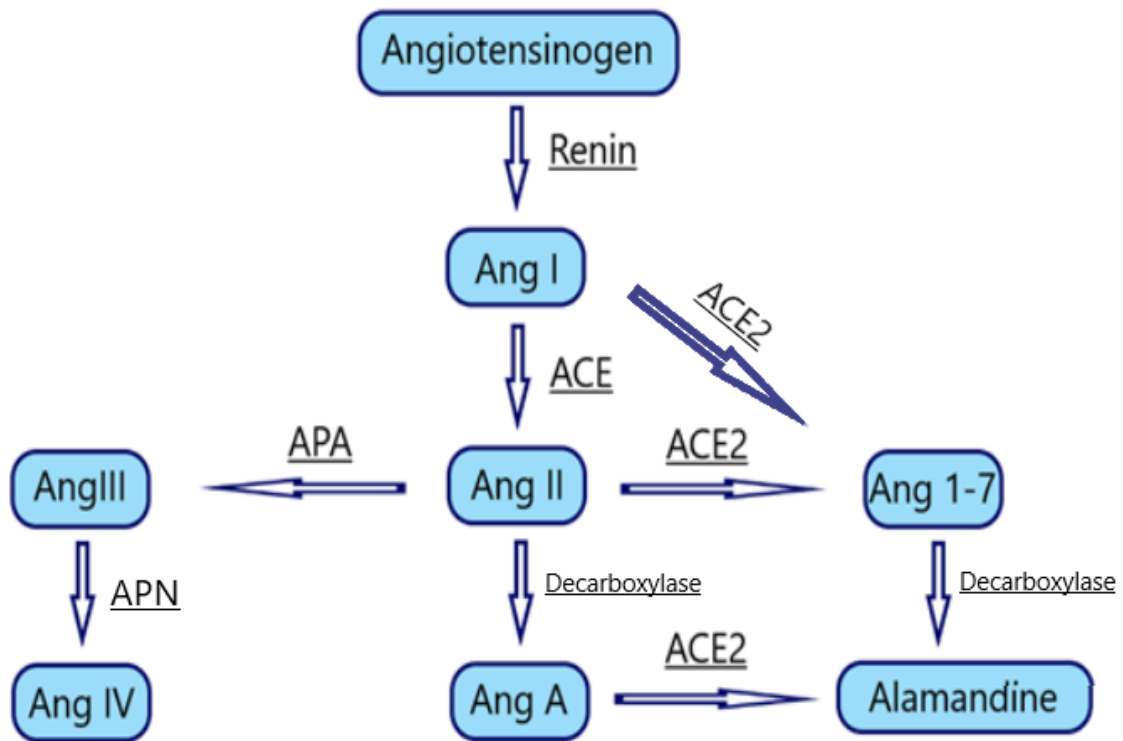


Figure 1. The renin-angiotensin system. Members of the renin-angiotensin system are shown, including the enzymes that contribute to the conversation of different members. Image was created using Microsoft Paint 3D.

Evidences have shown that RAAS not only functions in the circulating blood plasma, but it also has local paracrine, autocrine and intracrine effects in the tissues, also referred to as “tissue RAAS”. The activities of tissue RAAS have been described in various different organs and tissues including the nervous system, the kidneys, the gastrointestinal system, adipose tissues, and reproductive organs. Results suggest that the tissue RAAS is responsible for rather long-lasting, local effects complementing the actions of circulating RAAS (17).

1.5 The angiotensin type 1 receptor

1.5.1. The structure of AT1R

AT1R belongs to the GPCR superfamily, which is characterized by seven alpha-helix transmembrane domains (they are also called as 7-transmembrane receptors) that form three intracellular and three extracellular loops. The GPCRs represent one of the largest and most diverse protein families of the human genome. They can recognize a great variety of ligands, including, peptides, proteins, lipids, nucleotides, or small molecule chemicals, and they also play a role in light sensation. Ligands typically bind to their N-terminal extracellular loop, or in some cases to their transmembrane helices, such as rhodopsin-like family (18). There are numerous conserved regions in their structure, for instance, a conserved aspartate-arginine-tyrosine (DRY) sequence is present in their TM3 (19,20), and an asparagine-proline-X-X-tyrosine (NPXXY) region is found in TM7, playing a prominent role in their function, including AT1R. Their intracellular C-terminal domain is responsible for G protein binding and the initiation of downstream intracellular signal transduction. It contains numerous serine- and threonine-rich regions that can be phosphorylated by kinases, regulating the receptor functions (20).

GPCRs can be classified into six major groups, based on their structural characteristics and amino acid sequences: the rhodopsin family (family A), the secretin family (family B1), the adhesion family (family B2), the glutamate family (family C), cyclic-AMP receptors (class E), and the frizzled/taste family (family F). Among these, the most populous group of GPCRs is the rhodopsin-like receptors, comprising more than 700 proteins; AT1R is also a member of this family (21). Computational modeling data suggest that the binding of AngII to AT1R mainly involves the TM2-3-4-5-6-7 and the ECL2 loop. Experiments utilizing the mutagenesis of ECL2 loop suggest its critical role in AngII binding. It has been shown that significant interactions are forming between Val3 of AngII and Ile73 of AT1R, as well as between Asp1 of AngII and His83 of AT1R. Overall, it seems that the N-terminal region of AngII interacts with the extracellular domains of AT1R, while its C-terminal region fits into a pocket formed by transmembrane domains (22) (Figure 2.).

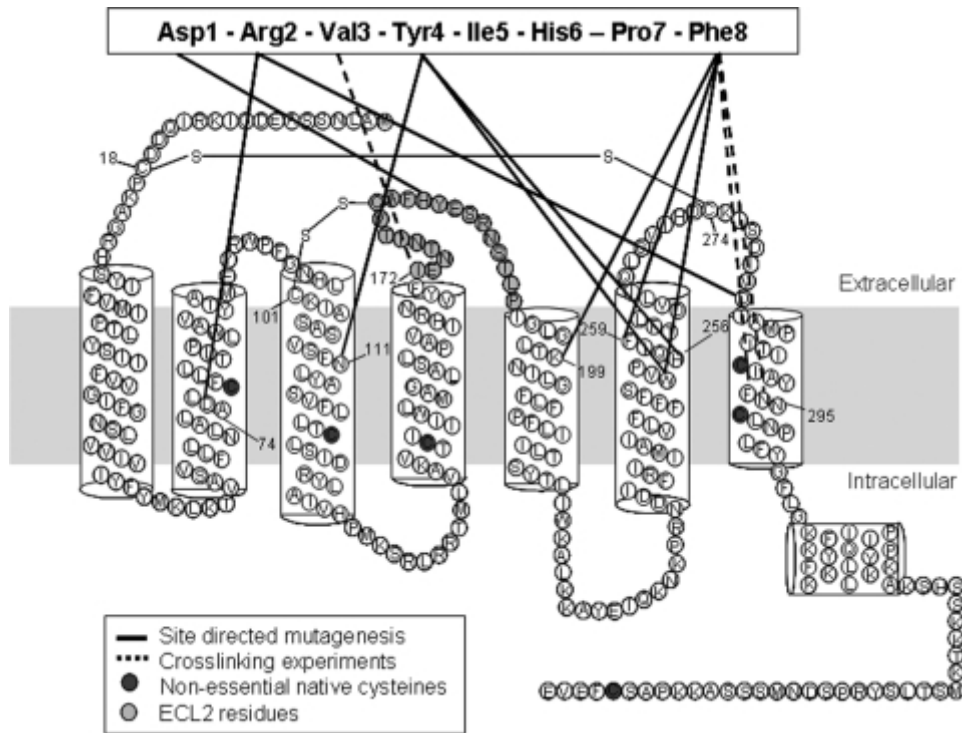


Figure 2. Structure of AT1R. Amino-acid sequence of the protein and the basic structure are shown. The figure is based on (22).

1.5.2. Activation of AT1R

AT1R can undergo conformational change from its inactive to active state not only by binding AngII, but also in response to other peptide or non-peptide ligands, which can serve as agonists for the receptor (23). Moreover, AT1R can also get activated by mechanical stress (24). It has also been described that GPCRs can function not just as monomers but they can also form homo- or heterodimers, and even oligomers. It was found that the AT1R can form homo- and heterodimers, as well. Factor XIIIa can play a role in the homodimer formation, making cross bindings with its transglutaminase activity. Heterodimer formation can either enhance or decrease the AT1R activity. It has been reported that AT1R can form heterodimers with numerous other GPCRs, for instance with AT2R, β -adrenergic receptors, Mas receptor, and various dopamine receptors. Furthermore, AT1R has been shown to form oligomers with other GPCRs (18,25)

1.5.3. Signal transduction of AT1R

The signal transduction mechanisms of AT1R can be categorized into two main types: G protein-dependent and G protein-independent pathways. In case of the G protein-dependent pathways, the AT1R initiates its signal transduction cascade by activating heterotrimeric G proteins. Its most important coupling is formed with the $G_{q/11}$ family, although interactions with $G_{i/o}$ - and $G_{12/13}$ proteins have also been described. The most prominent G protein-independent pathways involve the β -arrestin activation and the initiation of the JAK/STAT pathway. Furthermore, AT1R can also activate non-heterotrimeric, but monomeric (small) G-proteins, such as Ras, Rac or Rho (2,26).

1.5.3.1. G protein-dependent pathways

Heterotrimeric G proteins consist of α , β and γ subunits. The α -subunit possesses a GTPase enzyme activity and is capable to bind either GTP or GDP. In its inactive state, the α -subunit binds a GDP molecule and upon agonist activation of GPCRs GDP gets dissociated from the complex and exchanged to a GTP molecule. The GTP-bound α -subunit is responsible to mediate downstream signaling events, but also has GTPase activity, which can hydrolyze GTP to GDP. The $\beta\gamma$ -subunits remain linked together anchored to the plasma membrane. Most effects of the GPCRs are mediated by the α -subunit, although some signaling pathways can also be initiated from the $\beta\gamma$ -subunits (27).

The most significant effects of the AT1R are mediated by $G_{q/11}$ coupling. In that case, after the receptor activation by an agonist, the α -subunit interacts with phospholipase C- β (PLC β), which enzyme has the highest substrate specificity toward the phosphatidylinositol-4,5-bisphosphate (PI4,5P₂) lipid molecule. PLC β cleaves the plasma membrane PI4,5P₂ into diacylglycerole (DAG) and inositol-1,4,5-trisphosphate (IP₃) second messengers. DAG remains anchored to the plasma membrane and interacts with protein kinase C (PKC) as an activator of the enzyme. The PKC is a serine-threonine kinase that can catalyze the activation or inactivation of various intracellular target molecules, leading to various diverse effects; for example, it plays a role in receptor tyrosine-kinase activation and MAPK cascade activation. The soluble IP₃ activates its receptor (IP₃R) on the endoplasmic reticulum membrane. IP₃R functions as a ligand gated Ca²⁺ channel, and upon IP₃ binding, it allows Ca²⁺ release from the endoplasmic reticulum, leading to a cytosolic calcium signal. Ca²⁺ can bind to intracellular Ca²⁺

sensitive proteins, including the calmodulin. After binding Ca^{2+} , calmodulin activates numerous intracellular target proteins, including kinases or phosphatases, modulating many different cellular functions, like VSMC contraction or gene expression changes (2,26).

The activation of $G_{12/13}$ protein usually exerts its effects via activating small G proteins, typically Rho, and it is also able to activate phospholipase C and phospholipase D, furthermore it also has a role in the modulation of L-type Ca^{2+} channel function. In certain tissues, AT1R also binds to $G_{i/o}$ protein leading to the inhibition of adenylyl-cyclase and subsequent reduction in intracellular cAMP levels (26).

As it was mentioned above, AT1R is able to activate small G proteins either directly or indirectly through heterotrimeric G protein activation, as well. Among these, Ras can activate the Ras/Raf/MAPK pathway modulating different mitogenic responses, while Rho/Rho-kinase pathway plays an important role in VSMC function (28,29). Additional signaling pathways can be initiated from the $\beta\gamma$ -subunits, including the activation of protein kinase D and G protein-coupled receptor kinase 2 (GRK2) (27,30). Utilizing the G protein-dependent pathways, AT1R can transactivate growth factor receptors, such as EGFR and platelet derived growth factor receptor (PDGFR). These transactivations contribute to the activation of different MAPKs, regulation of gene expression changes, cell proliferation, migration, and apoptosis (31). The transactivation of EGFR will be discussed in detail later in subsequent chapters.

Furthermore, AT1R activation can lead to the production of different reactive oxygen species (ROS) by the activation of NADPH oxidase (NOX) enzymes. The ROS production plays a role in many different physiologic and pathophysiologic processes, such as inflammation, cell proliferation, apoptosis, and also contributes to the pathogenesis of different cardiovascular diseases (32–34).

1.5.3.2. G protein-independent pathways

The β -arrestins are intracellular adapter proteins playing a role in decoupling of the activated GPCRs from G proteins, and they are also responsible for the desensitization and internalization of GPCRs. Four members of the arrestin family have been discovered to date: arrestin1 and arrestin4 can be found only in the retina, whereas arrestin2 (β -arrestin1) and arrestin3 (β -arrestin2) can be found in almost every cell of the human body.

β -arrestins are very important elements in the regulation of ligand sensitivity of AT1R. The β -arrestins contain clathrin and activator protein (AP) 2 adapter-binding domains that initiate clathrin-coat mediated internalization of the ligand-bound receptor after its uncoupling from the G protein. Furthermore, β -arrestins can also serve as a scaffold in the formation of signal transduction complexes that plays a role in the initiation of MAPK cascade activation. It has been demonstrated utilizing a mutant AT1R, which was unable to bind G proteins, that MAPK activation can occur even in a G protein-independent way (18).

It has been described in various different cell types, including aortic smooth muscle and cardiac fibroblasts that AT1R can also activate JAK/STAT pathway, the main signal transduction pathway of cytokine receptors, primarily serving proinflammatory functions. The JAK/STAT pathway can be considered as a positive feedback for the AngII effect, since this pathway leads to increased AngII production. Moreover, the activation of the JAK/STAT pathway also increases the production of interleukin-6 and other cytokines that enhance the activity of this pathway (2).

1.6. The MAPK cascade

The MAPKs are serine/threonine kinases that regulate various cellular responses, including gene expression, proliferation, differentiation, and apoptosis. They are activated in response to a diverse array of stimuli, like mitogens, proinflammatory cytokines, heat shock, osmotic stress, and they also play a prominent role in the formation of long-term effects of AngII through AT1R activation (35). The mammalian MAPKs are classified to three subfamilies: extracellular signal-regulated kinases (ERKs), c-Jun N-terminal kinases (JNKs) and p38 mitogen activated protein kinases (p38 MAPKs). The ERK pathway is typically activated by mitogens and growth factors, whereas the JNK and p38 MAPK pathways are rather activated by inflammatory cytokines and cellular stress (36).

In their basal state, MAPKs are not active. They require activating phosphorylation within their activation loops that contain a threonine-X-tyrosine (T-X-Y) motif, and the activating dual phosphorylation happens on these threonine and tyrosine amino acids. The activated MAPKs are either translocated to the cell nucleus to affect gene expression regulation, or they can phosphorylate different target molecules in the

cytosol (36,37). Their inactivation is mediated by a special type of threonine-tyrosine phosphatases, called the dual-specificity phosphatases (DUSPs) (38). The characteristics of DUSPs will be discussed later in this thesis.

The MAPKs can be activated by various extracellular stimuli, including the activation of receptor tyrosine-kinases and GPCRs. The MAPK cascades are initiated with MAPK kinase kinases (MAPKKK) that phosphorylate MAPK kinases, which, in turn, can induce the activation of actual MAPKs by threonine and tyrosine phosphorylation. The ERK1/2 signaling is initiated by Raf protein that activates MEK1/2 in order to activate ERK1/2. The p38 and JNK pathways can be initiated by various MAPKKKs, such as MEKK1-4, MLKs, ASK or TAK1. In the case of p38 MAPK, the MAPKK's role can be fulfilled by MEK3/6 or MEK4, whereas the JNK is usually phosphorylated by MEK4/7 (Figure 3.) (36).

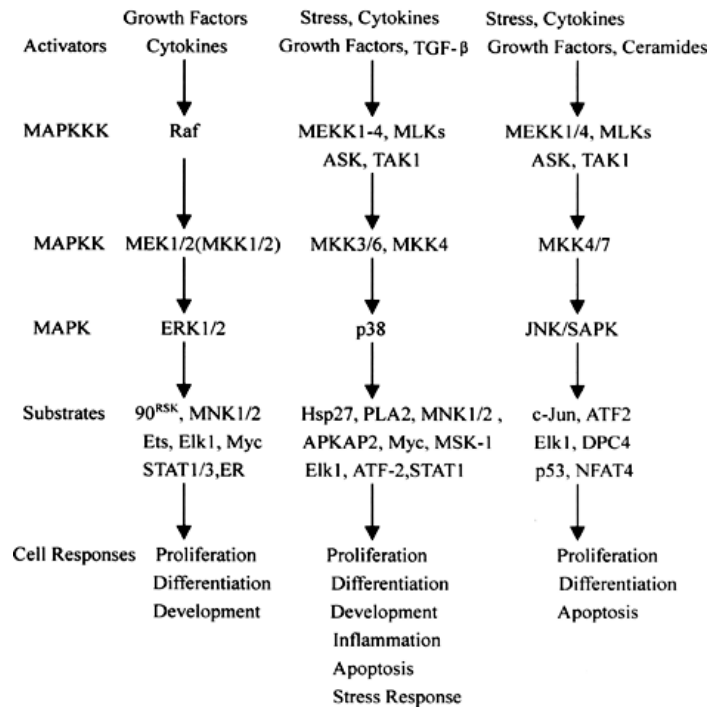


Figure 3. MAPK cascades. Activation and physiological effects of ERK1/2, p38 and JNK pathways. This figure is based on (36).

In the case of AT1R, similarly to other G_{q/11} coupled receptors, MAPKs can be activated through different signaling pathways. Stimulation of AT1R activates different small G proteins that can induce MAPK cascades. Additionally, PKC can also directly initiate phosphorylation cascades leading to the activation of ERK1/2 and JNK. The production of DAG and the cytosolic calcium signal also lead to the activation of Rap1,

which in turn initiates either ERK1/2 or ERK5 signaling. In a calmodulin-dependent way, any increase of cytosolic Ca^{2+} concentration also contributes to the activation of small G-proteins, including Rac, Ras and R-Ras, which in turn can initiate ERK1/2, JNK and p38 pathways, as well. In addition, AngII is capable of inducing ROS production in VSMCs and ROS molecules, which in turn, enhances MAPK activation. It was described that ROS production mainly activates ERK1/2 and JNK pathways, although they do not appear to significantly impact p38 MAPK activation. The AngII mediated transactivation of growth factor receptors, like EGFR and PDGFR also plays a crucial role in AngII-induced MAPK activation in vascular smooth muscle cells. The EGFR transactivation of AT1R will be discussed in more details later in this thesis (39,40).

In VSMCs MAPKs exert their effect in the nucleus, mainly modulating gene expression changes that lead to cell proliferation, hypertrophy, cell migration, increase of collagen production and hypercontractility. These changes are all essential in the pathological vascular remodeling, thus AngII mediated MAPK activation strongly contributes to the pathogenesis of RAAS related chronic cardiovascular diseases, like hypertension or atherosclerosis (39).

1.7. Dual-specificity phosphatases

Dual-specificity phosphatases (DUSPs), also known as MAPK-phosphatases (MKPs) are among the most important regulators of different MAPKs. It has been established that they are not only capable to inactivate the active, phosphorylated MAPKs by removing the phosphate groups from threonine and tyrosine amino acids, but they can also bind to inactive MAPK isoforms, thereby making them unavailable for their activation by upstream kinases (41,42).

On a structural level, they are made up of an N-terminal non-catalytic and a C-terminal catalytic domain. The C-terminal active-site shares highly conserved His-Cys-x-x-x-x-Arg-Ser motif with other members of the protein tyrosine phosphatase (PTP) superfamily, thus this domain does not provide strict selectivity towards the potential substrates. The N-terminal kinase-interacting motif (KIM) or MAP kinase-binding (MKB) domain contains clusters of positively charged and hydrophobic amino-acids that determine their binding specificity and facilitate the interaction with their substrates. Some DUSP isoforms lack of KIM/MKB domain, though have less specificity for certain

substrates. These ones form the so called group of atypical DUSPs including DUSP3, DUSP11, DUSP12, DUSP13, DUSP14, DUSP15, DUSP17/19, DUSP18/20, DUSP21, DUSP22, DUSP23/25, DUSP24, DUSP26, DUSP27, and DUSP28. Those DUSP isoforms that contain KIM/MKB domain are classed as typical DUSPs and further divided to three subgroups based on their localization. Typical type I DUSPs (DUSP1, DUSP2, DUSP4, DUSP5) are localized in the nucleus, typical type II DUSPs (DUSP6, DUSP7, DUSP9) are cytosolic enzymes, while typical type II DUSPs (DUSP8, DUSP10, DUSP16) are present in both in nucleus and cytoplasm as well (Table 1.) (43,44).

Table 1. Groups of dual specificity phosphatases.

Group	Substrate	Isoforms
I. Typical nuclear	ERK1/2, sometimes p38 and/or JNK	DUSP1, DUSP2, DUSP4, DUSP5
II. Typical Cytosolic	Highly ERK1/2 sensitive	DUSP6, DUSP7, DUSP9
III. Typical Nuclear/Cytosolic	Mainly p38 and MAPK	DUSP8, DUSP10, DUSP16
IV. Atypical	Various substrates, including non-MAPK proteins	DUSP3, DUSP11- DUSP15, DUSP18- DUSP24, DUSP26, DUSP27

Our research group has demonstrated that AngII can upregulate various different DUSP isoforms in VSMCs, most significantly the DUSP4, DUSP5, DUSP6 and DUSP10 isoforms (Figure 11.). During our research, we further investigated the exact mechanisms of the AngII mediated DUSP5, DUSP6 and DUSP10 upregulation. We discovered that in case of all the three isoforms, AngII stimuli caused upregulation via AT1R activation through G_{q/11} mediated Ca²⁺ release, though in case of DUSP10, the role of PKC activity also played a contributory role. It was also demonstrated that in the upregulation of DUSP5 and DUSP6, the activation of p38 MAPK plays a significant role (data was presented in another PhD candidate's dissertation). Based on pathway activity analysis, EGFR transactivation seemed to have a prominent role in AngII mediated gene expression changes. In the second part of this thesis, I will characterize and discuss the

importance of EGFR transactivation and its role in the AngII mediated *DUSP5*, *DUSP6* and *DUSP10* upregulation in VSMCs.

DUSP5 is an approximately 42 kDa protein and is localized in the nucleus. In contrast to other nuclear DUSP isoforms, that have usually broad activity towards different MAPKs, DUSP5 is highly specific for the ERK1/2. It was shown in many cell lines that ERK1/2 itself induces the transcription of DUSP5 through Elk1/2 activation, so it can work as a negative feedback regulation for ERK1/2. However, in our studies, performed on primary rat VSMCs, the AngII mediated DUSP5 upregulation seemed to be also dependent on the p38 pathway. It has been described that DUSP5 is highly expressed in angioblasts and has an essential role in cardiovascular development. Other studies reported that DUSP5 plays a cardioprotective role by preventing ERK1/2 mediated cardiac hypertrophy and fibrosis. In brain vessels, DUSP5 was described to have a crucial role in the autoregulation and myogenic responses in brain vessels, though there is no extensive data on the exact vascular effects of DUSP5 (45).

DUSP6 is a type II DUSP, acting primarily in the cytosol. Similarly to DUSP5, DUSP6 is also highly specific to ERK1/2 and has no relevant role in the regulation of p38 or JNK pathways. There is limited data about the exact role of DUSP6 in the physiological and pathophysiological role of DUSP6 in the cardiovascular system, but recent studies indicate that DUSP6 deficiency or DUSP6 inhibition can be protective after myocardial infarction (45).

DUSP10 is a type III DUSP that can be found in both the cytosol and the nucleus. Unlike DUSP5 and DUSP6 isoforms, DUSP10 preferentially dephosphorylates JNK and p38 MAPKs. DUSP10 carries an N-terminal extension, the function of which is not fully understood; though it may be involved in the determination of the intracellular localization of the protein (45). Currently, there is limited information on the physiological and pathological roles of DUSP10 in vascular smooth muscle cells.

1.8. AngII mediated EGFR transactivation

AT1R can activate the MAPK cascades through multiple ways, including the transactivation of growth factor receptors. The transactivation of EGFR has been shown to play a significant role in the amplification of AngII-mediated long-term effects in vascular smooth muscle cells (4).

1.8.1. The EGFR

The EGFR belongs to the ErbB receptor family of receptor tyrosine kinases that has a special importance in oncology (46,47). However, EGFR was also reported to play a role in the pathogenesis of different non-neoplastic diseases like psoriasis or asthma (48,49). The activation of EGFR usually causes proliferative effects in cells, it promotes cellular hypertrophy, migration and was also described to play a role in cellular senescence and in pro-inflammatory processes (50).

EGFR can be activated by numerous different ligands but the most significant ones are the EGF and transforming growth factor- α (51). The ligand binding of EGFR results in homo- or heterodimerization, followed by autophosphorylation by the cytosolic tyrosine-kinase domains. The phosphorylated residues serve as binding sites for different SH2 domain containing signal transducer molecules, including GRB2, which initiates the Ras-Raf-MAPK pathways. Other important pathways activated by EGFR are the PI3K-Akt, the PLC γ , and the STAT signaling pathways (50,52).

1.8.2. Transactivation of EGFR by AT1R activation

Numerous GPCRs have an ability to transactivate EGFR in a ligand-dependent manner, mainly through the release of membrane-anchored ligands, cleaved by ADAM (a disintegrin and metalloproteinase) family metalloproteinases. In case of AT1R, the G $_{q/11}$ pathway leads to the activation of the metalloproteinase ADAM17, which clusters in caveoles with EGFR and Hb-EGF. The active ADAM17 cleaves Hb-EGF and the released domain can bind to the EGFR as an activatory ligand (4).

It has also been observed that $\beta\gamma$ -subunits of different G proteins can induce ligand-independent EGFR transactivation via recruitment of β -arrestins or c-Src kinase. Many GPCRs, including AT1R, are able to form a heterocomplex by direct protein-protein interaction with EGFR. It was reported that EGFR-AT1R heterodimerization can recruit Grb2 that results in the initiation of different downstream pathways (4).

1.9. LMCD1

LIM and cysteine-rich domains 1 (LMCD1), also known as Dyxin is a member of the LIM protein family. LIM proteins have diverse functions in cellular physiology,

mainly involved in regulation of gene expression, cytoskeletal function, and cell fate determination (53–55). LIM proteins are defined as modulators of GATA (Glycine-Adenine-Thymine-Adenine) function, which is an important factor in tissue development and differentiation, especially in cardiac, pulmonary and hematopoietic tissues (53,55). Structurally, LMCD1 contains two LIM domains at the C-terminus, a cysteine-rich domain at the N-terminus and a PET (Prickle, Espinas and Testin) domain in the central part. LIM domains contain conserved zinc-binding residue that can establish zinc-finger structures. There are a limited number of studies so far concerning the exact function of LMCD1. It has been described that LMCD1 acts as a repressor for GATA6, as it inhibits its DNA binding in lung epithelium, cardiac myocytes and vascular smooth muscle cells (53). In the heart, it has also been reported that LMCD1 provokes cardiac hypertrophy, in cardiac myocytes augmented cell growth and fibrosis was observed (56). In vascular smooth muscle cells, it was observed that thrombin significantly increases the expression LMCD1 via $G_{q/11}$ activation that promotes vascular smooth muscle proliferation and atherogenesis (57,58).

Our results suggest that in primary rat VSMCs, AngII also upregulates *LMCD1* expression. The exact mechanisms leading to AngII mediated *LMCD1* upregulation, as well as the functional consequences and its functions in these cells will be discussed as one of the main cornerstones of this thesis.

2. Objectives

The aim of this PhD research was to investigate genes that exhibit upregulation in response to AngII stimulation in primary rat vascular smooth muscle cells, with a particular focus on the role of EGFR transactivation mediated by the AT1R. The objectives are organized into two major areas:

2.1. Aims related to AngII-mediated gene expression changes:

- To identify genes that are significantly upregulated by AngII in primary rat VSMCs.
- To elucidate the signaling mechanisms leading to the AngII-mediated upregulation of *LMCD1*
- Characterization of the physiological effects of LMCD1 in VSMCs.

2.2. Aims related to EGFR transactivation:

- Silencing *EGFR* with a lentiviral vector system effectively in primary rat VSMCs.
- To examine the effects of *EGFR* silencing on AngII-induced upregulation of *DUSP5*, *DUSP6* and *DUSP10* compared to pharmacological EGFR inhibition.

3. Methods

3.1. Materials

For cell culturing, plates and dishes were purchased from Greiner (Kremsmunster, Austria). Most reagents for cell culture and molecular biological experiments were obtained from ThermoFischer Scientific (Waltham, MA, USA), except the following materials: AngII, EGFR inhibitor AG1478, calcium chelator BAPTA-AM, CaMKII inhibitor CK59, MEK inhibitor PD-98058, p38 inhibitor SB-202190, JNK inhibitor SP-600125, and FAK/Pyk2 inhibitor PF-562271 were purchased from Sigma-Aldrich (St. Louis, MO, USA). The G_{q/11} inhibitor YM-254890 was ordered from WAKO-Chemicals (Neuss, Germany). Fast Start Essential DNA Green Master Mix was obtained from Roche (Basel, Switzerland). Anti-phospho-EGFR (Cat.no.: 2236S), anti-mouse-HRP (Cat.no.: 7076S), and anti-rabbit-HRP (Cat.no.: 7074S), antibodies were purchased from Cell Signaling (Danvers, MA, USA). Anti-LMCD1 antibody (Cat.no.: ab-179454), was from Abcam (Cambridge, UK). Anti- β -actin antibody (Cat.no.: A1978) was purchased from Sigma-Aldrich (St. Louis, MO, USA). Fluorescent antibodies used in western blot assays were obtained from Azure Biosystems (Anti-mouse fluorescent antibodies, Cat.no.: AC2129 and AC2135), (Dublin CA, USA). All other antibodies used for the experiments presented in this thesis were purchased from ThermoFischer Scientific (Cat.no.: AlexaFluor 488 anti-rabbit – A11034; AlexaFluor 568 anti-mouse – A11031; Anti-Golgin-97 – A21270, Anti-GM130 - MA5-47668), (Waltham, MA USA).

3.2. Cell cultures

Most experiments were performed on primary rat VSMCs, isolated from the aorta thoracalis of 40-60-day-old male Wistar rats. Animals were purchased from Charles River Laboratories and housed at Semmelweis University, Budapest. All animal procedures were approved by the Animal Care Committee of the Semmelweis University, Budapest and the relevant Hungarian authorities (No. 001/2139-4/2012) and adhered to legal and institutional guidelines for animal care. The investigation complies with the Guide for the Care and Use of Laboratory Animals (NIH, 8th edition, 2011). Animals were sacrificed by decapitation, then the aorta thoracalis was removed and cleaned from tissue remains.

The vessels were cut into 1-2 mm wide sections, then incubated with collagenase. The digested sections were placed on a sterile plate in DMEM medium (Biosera, Nuaille, France) completed with 10% FBS (Biosera, Nuaille, France), 1% Glutamax (Gibco, Dublin, Ireland), and 1% penicillin-streptomycin (Lonza, Gampel, Switzerland). Experiments were performed using cells at passage 3.

Experiments involving LMCD1 overexpression were performed on A7r5, an immortalized rat vascular smooth muscle cell line. Lentiviral particles were produced using HEK293T cells.

3.3. Plasmid constructs

3.3.1. LMCD1 Overexpressing plasmid constructs

For LMCD1 overexpression, a pcDNA3.1 plasmid was used, that was designed to express HA-tagged LMCD1 protein. To enhance the complete open reading frame of LMCD1, cDNA obtained from vascular smooth muscle cells (VSMCs) treated with AngII for 2 hours was utilized as the template. The initial PCR product was separated by electrophoresis, was purified using the GeneJet Gel Extraction Kit (Thermo Fisher Scientific), and then subjected to a second round of PCR with primers containing restriction enzyme sites.

3.3.2. *EGFR* silencing and lentivirus production

To silence *EGFR* gene, lentiviral constructs were used, expressing *EGFR* specific short hairpin RNA (shRNA). shRNAs are able to silence a specific gene via RNA interference. The antisense (guide) strand of the shRNA directs the RISC complex (RNA-induced silencing complex) to the complementary sequence, causing the degradation or the failure of translation of the complementary mRNA (58). The expressed shRNA sequences were delivered into the VSMCs through lentiviral particles. Lentiviruses were produced in HEK293T cells. Cells were co-transfected with pLKO.1 puro transfer, pCMV-VSV-G envelope, and pCMV-dR8.2 packing plasmids, using calcium-phosphate precipitation method. For each plate of HEK293T cells, transfer, envelope and packing plasmids were mixed into 450 μ l of sterile distilled water, then 50 μ l of 2.5 M calcium-chloride solution was added. The mixture was added dropwise to 500 μ l of 2x HEPES-

buffered solution (42 mM HEPES, 15 mM D-glucose, 1.4 mM Na₂HPO₄, 10 mM KCl, 274 mM NaCl 274 mM, pH 7.1). The final mixture was added dropwise to the cells, then the medium was changed after 6 hours with fresh complete DMEM. 48 hours after the transfection, the lentiviral particle containing supernatant was collected, then it was centrifuged (10 minutes at 3000 *rpm*), then poured into a clean tube. Next, supernatants were filtered through a Merck's sterile Millex syringe driven filter unit (0.22µm) into another sterile tube. The purified lentiviral samples were concentrated using the Lenti-X Concentrator kit (Takara-Bio, Kusatsu, Japan) following the manufacturer's instructions. Viral titer was measured using abm's qPCR lentivirus Titration Kit following the manufacturer's instructions. Samples were stored at -80 °C.

3.4. Affymetrix GeneChip Assay

Following serum deprivation, vascular smooth muscle cells (VSMCs) were treated with 100 nM AngII for 2 hours at 37 °C, after which the cells were lysed using Trizol reagent. The RNA sample quality was assessed with an Agilent BioAnalyzer RNA Nano lab chip prior to conducting the array experiments. Total RNA extraction and analysis using the Affymetrix Rat Gene 1.0 ST GeneChip Array (Affymetrix, Santa Clara, CA, USA) were carried out by UD-GenoMed Medical Genomic Technologies Ltd., based at the University of Debrecen in Hungary. Hybridization and image scanning followed the protocols established by UD-GenoMed Medical Genomic Technologies Ltd. The microarray experiment was conducted in triplicate. Raw CEL files underwent background correction and normalization using the oligo R package, while differential expression analysis comparing Angiotensin II to the vehicle control was performed using the limma R package. We utilized the PROGENy pathway activity analysis tool to assess the changes in pathway activity by AngII. The calculated PROGENy pathway activity scores were normalized against a null distribution (generated through 10,000 random permutations of gene names) to derive pathway activity z-scores.

3.5. Plasmid transfection

LMCD1 was overexpressed using lipofectamine based transfection. Lipofectamine 2000 transfection reagent was obtained from Thermo Fischer (Waltham, MA, USA). Transfection protocol was performed on A7r5 cells, following the

manufacturer's instructions. Approximately 200,000 A7r5 cells were plated on 6-well plates, one day prior to transfection and the cells were used for experiments 2 days after the transfection.

3.6. Lentiviral infection

Approximately 200,000-250,000 VSMCs were seeded onto 6-well plates one day prior to infection. Equal titers of lentiviral preparations were diluted in complete DMEM, containing 1% Glutamax and 8 µg/ml PolyBrene (Sigma Aldrich). The cell culture medium was replaced 24 hours later. Cells were subjected to experiment 48 hours after the lentiviral infection.

3.7. Stimulation and pharmacological inhibitor treatments

VSMCs (200,000-250,000/well) were serum-deprived overnight or for 16-48 hours, depending on the experimental requirements. In case of examination of kinetic changes over time, cells were stimulated for varying durations. For agonist stimulations, the following concentrations were used: 100 nM AngII, 50 µg/ml EGF, 1µM AVP, or 3 µM TRV120023. In case of experiments performing inhibitor pretreatments, cells were incubated with serum-free DMEM containing the recommended concentration of the specific pharmacological inhibitor for 10-30 minutes before the hormonal stimulation. In these experiments, 2-hour-long agonist simulations were performed.

3.8. Gene expression measurements

All gene expression measurements were done with real-time quantitative PCR method. After treatment, RNA was isolated from the cells with RNeasy Plus Mini kit from Qiagen (Hilden, Germany) following the manufacturer's instructions. Then the RNA concentrations were measured with the spectrophotometric method, using NanoDrop OneC (ThermoFischer Scientific, Waltham, MA, USA). cDNA was synthesized from the mRNA using RevertAid Reverse Transcription Kit according to the manufacturer's instructions (ThermoFisher Scientific).

For real-time quantitative PCR measurements LightCycler 480 SYBR Green I Master kit (Roche, Basel, Switzerland) was used. To determine the expression levels of

the examined genes, relative quantification was applied and the normalization was against house-keeping gene glyceraldehyde-3-phosphate dehydrogenase (*GAPDH*). For measuring fluorescent data, LightCycler 480 system (Roche) was used. qRT-PCR primers were obtained from Sigma-Aldrich, their sequences are listed in Table 1. The following thermal cycling protocol was performed: 5 minutes pre-incubation at 95°C, followed by 45 cycles of amplification (10 seconds at 95°C, 5 seconds at 62°C and 15 seconds at 72°C), then a melting curve, that starts at 95 °C for 5 seconds, then 1 minute at 65 °C and 97 °C and cooling 30 seconds at 40 °C. The following equation was used to calculate fold ratios of gene expressions: $\text{Ratio} = E^{\Delta C_t \text{ target gene}} / E^{\Delta C_t \text{ GAPDH}}$.

Table 2. qRT-PCR primer sequences.

Gene name	forward primer (5'→ 3')	reverse primer (5'→ 3')
<i>Gapdh</i>	CCTGCACCACCAACTGCTTAG	CAGTCTTCTGAGTGGCAGTGTGATG
<i>Dusp5</i>	GGCAAGGTCCTGGTTCACTGT	GTTGGGAGAGACCACGCTCCT
<i>Dusp6</i>	ATCACTGGAGCCAAAACCTG	CGTTCATGGACAAGTTGAGC
<i>Dusp10</i>	GGCAAAGAACCCTGGTATT	AGAAACAGGAAGGGCAGGAT
<i>LMCD1</i>	CCTCGAGTGCAAAAGATGTCC	AATTTTCCGATCATCCTCCA

3.9. Immunostaining

Cells were seeded into 8-well ibidi plates for immunostaining (10,000 cells/well), then treatment protocols were performed. After treatments, cells were fixated with 4% paraformaldehyde solution in PBS. After fixation, cells were treated with 0.1% Triton X-100 solution (in PBS) for permeabilization, and autofluorescence was reduced by incubation in 0.1% sodium-borohydride. Cells were blocked in 5% BSA in PBS, then stained with primary and fluorescent secondary antibodies. Nuclei were stained with To-Pro reagent (Invitrogen, Waltham, MA, USA) according to the manufacturer's instructions. Imaging was performed using Zeiss LSM 710 confocal microscope (Zeiss AG, Jena, Germany), and analyzed with ImageJ software 1.53e.

3.10. Western blot assay

Western blot assays were performed to measure protein expressions. Cells were lysed in Laemmli SDS sample buffer, completed with protease and phosphatase inhibitors, then prepared with sonication. The samples were loaded onto SDS-polyacrylamide gels for electrophoresis, then transferred to PVDF membranes using the Trans-Blot Turbo Transfer System by Bio-Rad Laboratories (Hercules, CA, USA). Membranes were blocked in PBST containing 5% non-fat milk, then incubated with primary, then secondary antibodies. Secondary antibodies were either fluorescent or HRP-linked. In case of HRP-linked secondary antibodies, ECL chemiluminescent substrate reagents were used for signal detection (Immobilion Western HRP substrate reagent, Millipore, Billerica, MA). Both chemiluminescent and fluorescent signals were detected using Azure c600 system (Azure Biosystems, Dublin, CA). The intensities were quantified by densitometry with ImageJ software 1.53e.

3.11. ³H-Leucine incorporation assay

To determine cellular growth, ³H-leucine incorporation assay was performed. A7r5 cells were plated on a 24-well plate (20,000-30,000 cells/well), then transfected with either LMCD1 overexpressing pcDNA plasmids or empty pcDNA plasmids (control group). One day after the transfection, cells were treated with ³H-labeled leucine containing serum-free DMEM solution. After 24 hours, cells were washed twice with ice-cold PBS and treated with 5% trichloroacetic acid (TCA) for 30 minutes. The TCA was removed, and the cells were washed twice with PBS, and 0.5 ml 0.5 M NaOH was added to the wells and incubated at room temperature for 30 minutes. Samples were collected into 10 ml of OptiPhase HiSafe 3 scintillation cocktail (PerkinElmer, Inc; Waltham, MA, USA). Wells were further rinsed with additional 100 µl of distilled water, which was also added to the scintillation vials. Radioactivity of the samples were measured using Packard Tri-carb Liquid scintillation Counter 2500 TR scintillation reader, alongside a blank control sample containing only distilled water in the scintillation cocktail.

3.12. Wound-healing assay

Migration capability of the cells were assessed with wound-healing assay. A7r5 cells were plated into 3 cm-diameter plates, then transfected with either LMCD1 overexpressing or empty pcDNA plasmids. The cell monolayer was scraped with a sterile 200 µl pipette tip on the following day. The wounds were photographed with Leica DMI6000B (Leica, Wetzlar, Germany) microscope at 5x magnification. 48 hours after the scratching, the wounds were photographed again at the identical positions. The areas of the photographed wounds were measured with ImageJ software.

3. 13. Statistical analysis

Statistical analysis was performed using GraphPad Prism 6, 8 and 9 softwares. In case of real-time q-PCR measurements, performing samples treated with agonist stimulation and also pretreated with pharmacological inhibitors or infected with lentiviral particles were evaluated using multiple linear regression. One-way ANOVA test was performed for the evaluation of real-time q-PCR measurements done on samples which received only agonist stimulation or only virus infection. For the statistical analysis of ³H-leucine incorporation assay and wound-healing assay, paired t-test was used.

4. Results

4.1. Gene expression changes in VSMCs to AngII stimulation

4.1.1. Affymetrix gene-chip assay

Affymetrix Gene Chip Rat Gene 1.0 ST array was utilized using primary rat VSMCs at passage 2 to identify genes that are up- or downregulated by AngII stimuli in primary rat VSMCs. The VSMCs were stimulated with 100 nM AngII or vehicle for 2 hours. Using the limma package, differential expression analysis was performed between AngII and vehicle treated samples. As shown in the volcano plot, AngII caused significant upregulation of 74 genes (false discovery rate, based on the Benjamini–Hochberg correction < 0.05 , \log_2 fold change > 1), including *LMCD1* (Figure 4.). Given that *LMCD1* is a relatively poorly examined gene, previously described to play a role in different proliferative processes, we decided to characterize this gene in the context of VSMC physiology and in mediating the long-term effects of AngII.

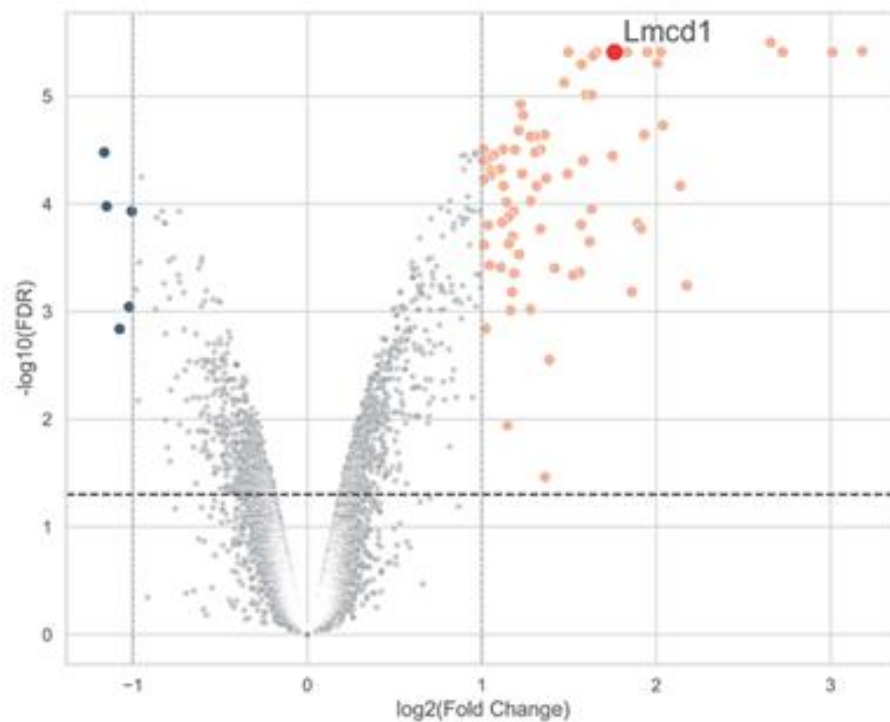


Figure 4. Gene expression and pathway analysis of the response of primary VSMCs to AngII stimulation. Differential gene expression in VSMCs is shown at the volcano plot

VSMCs were treated for 2 hours with 100nM AngII beside a control group incubated with vehicle. On the x-axis, the log₂ fold change in gene expression is presented, while the y-axis shows the $-\log_{10}$ of the false discovery rate (FDR). The horizontal dotted line marks the significance threshold, where FDR < 0.05. The color highlight labels the genes which one's log₂ fold change is greater than 1, either up- or downregulated by AngII. *LMCD1* gene is labeled with a red dot.

4.2. AngII-mediated upregulation of *LMCD1* in VSMCs

4.2.1. Kinetic changes over time of *LMCD1* gene and protein expression in response to AngII

The Affimetryx gene chip-assay show that *LMCD1* is among the genes that are significantly upregulated by AngII stimulation in VSMCs. Although the gene-chip assay was performed using a 2-hour AngII stimulation, we wanted to determine the detailed the kinetic changes over time of the *LMCD1* gene, and also the *LMCD1* protein expression changes in VSMCs in response to AngII treatment. In order to examine gene expression changes, after overnight serum depletion, the VSMCs were stimulated with 100 nM AngII and samples were collected at hourly intervals over a 6-hour period and analyzed using real-time quantitative PCR. As it is shown in Figure 5.A, *LMCD1* mRNA levels increased dramatically after 1 hour and remained elevated in the first three hours, then started to decrease after the third hour. Based on these results, we used a 2-hour AngII stimulus for further gene expression studies.

The time course of protein expression were determined using both western blot assay (Figure 5.B) and immunostaining (Figure 5.C). Both methods suggested that the protein expression of *LMCD1* peaks around 24 hours following AngII treatment and reduces close to the baseline level after 48 hours.

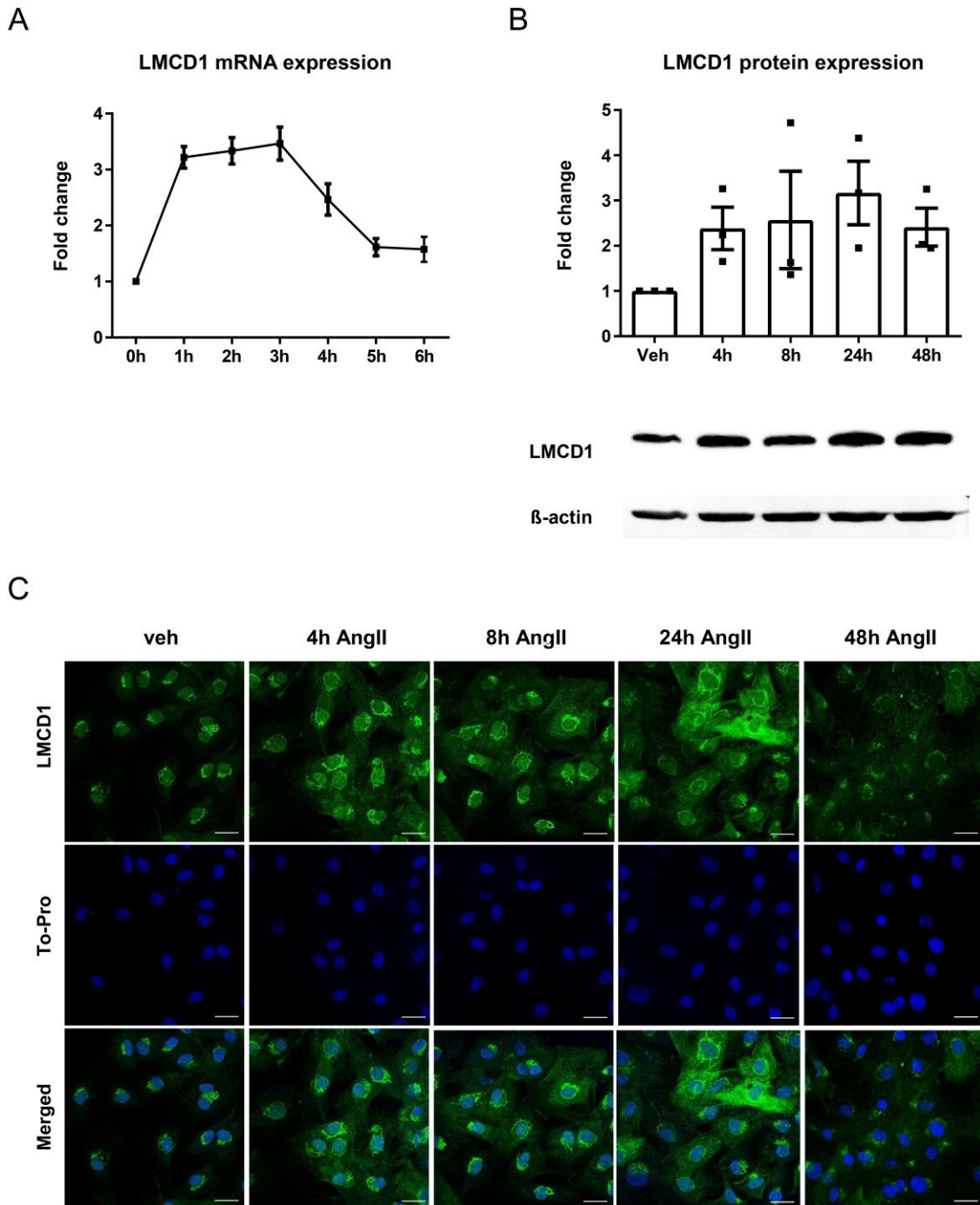


Figure 5. Kinetic changes over time of AngII-induced LMCD1 gene and protein expression. VSMCs were serum-starved overnight prior to treatment with 100 nM AngII. (A) Cells were stimulated with AngII every hour for 6 h, and then mRNA was isolated from samples. The expression of *LMCD1* was measured using quantitative real-time PCR, with standardization against the *GAPDH* housekeeping gene. Mean values \pm SE are presented ($n = 5-6$). (B) *LMCD1* protein expression was measured using immunoblot assay. Cells were treated with AngII for various time periods between 0 and 48 h. The membranes were labeled with either anti-*LMCD1* primary antibody or anti- β -actin (loading control). HRP-linked or fluorescent secondary antibodies were used for

detection (a representative immunoblot record is shown in the lower part of the graph). Protein levels were normalized to unstimulated (0 h) samples. Mean values \pm SE are shown ($n = 3-4$). (C) Cells were treated with AngII for various time periods between 0 and 48 h. Samples were fixed with paraformaldehyde and stained with an anti-LMCD primary antibody and an AlexaFluor488-labeled secondary antibody (green). Nuclei of cells were stained with To-Pro reagent (blue). Immunofluorescent signals were examined using a Zeiss LSM710 confocal laser-scanning microscope. Scale bars represent 25 μ m.

4.2.2. Intracellular localization of LMCD1

Based on observations from previous experiments, we sought to determine in which cell organelles LMCD1 is located. Fluorescent confocal microscopy images suggested that LMCD1 seems to be accumulated in the nuclei and the Golgi-apparatus. In order to prove this hypothesis, specific labeling of nucleus, trans- and cis-Golgi was used after 24 hours of AngII stimulation, and the colocalization with LMCD1 was evaluated. Based on the confocal images, a clear colocalization was observed with the nucleus, the cis- and trans-Golgi (Figure 6.), indicating that LMCD1 is primarily localized to these regions. Interestingly, no mention has been made in the literature of LMCD1 being localized in the Golgi-apparatus so far, it is mainly described to be localized in the nucleus and cytoplasm (53).

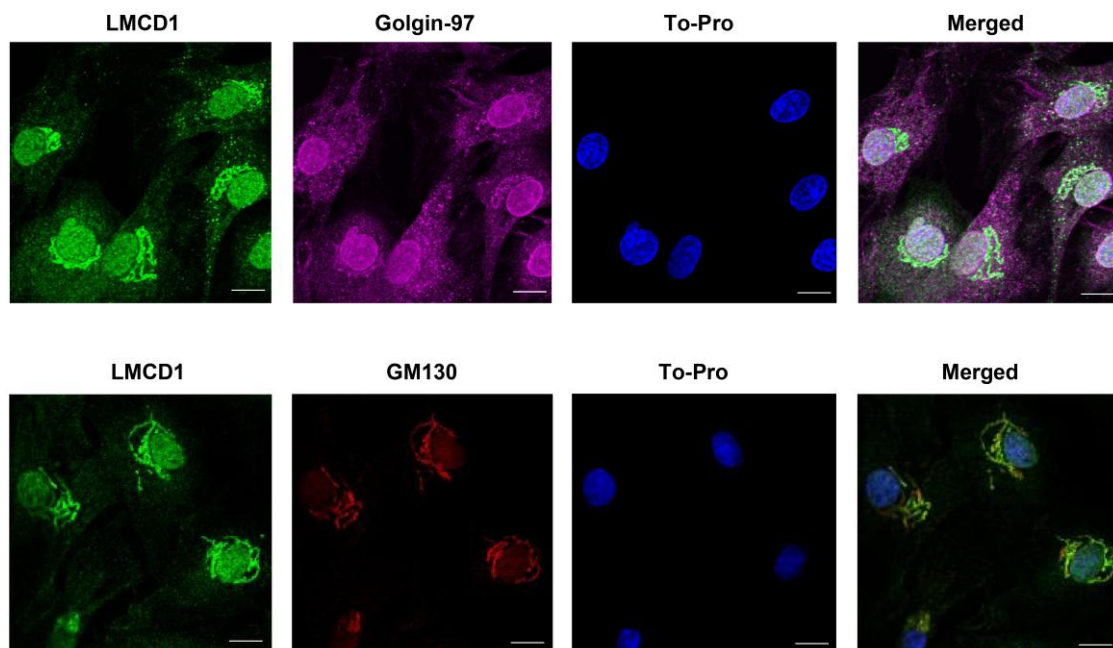


Figure 6. Intracellular localization of LMCD1. VSMCs received overnight serum-depletion, then were treated with 100 nM AngII for 24 hours, thereafter fixed in 4% PFA

solution. Immunofluorescent confocal images are shown. Anti-LMCD1 staining (green), anti-golgin-97 staining (magenta), anti-GM130 staining (red), To-pro nuclear staining (blue) and merged images are shown. Scale bars represent 25 μm

4.2.3. Role of AT1R and G-protein coupling in AngII mediated LMCD1 expression

In order to determine the dominant signaling mechanisms leading to *LMCD1* upregulation in response to AngII stimulation, we had to find out which receptors of AngII were involved in the signaling. We used Candesartan, an AT1R specific inhibitor, to examine the role of AT1R in AngII-mediated *LMCD1* upregulation in VSMCs. Cells pretreated with Candesartan were not able to increase *LMCD1* mRNA expression in response to AngII stimulation, the mRNA level of *LMCD1* was similar to unstimulated cells (Figure 7.A). This result suggests that AngII mainly exerts its *LMCD1* upregulating effects by AT1R activation. As it was described in the introduction, AT1R is capable of initiating numerous different signaling pathways, in addition to $G_{q/11}$ mediated effects. YM-254890 is a selective $G_{q/11}$ protein inhibitor. In cells pretreated with YM-254890, the AngII was not able to upregulate *LMCD1* expression levels, which supports the importance of $G_{q/11}$ coupling in this process (Figure 7.B). The importance of $G_{q/11}$ protein is also supported by the fact that AVP, a vasoconstrictor hormone, which acts via a $G_{q/11}$ coupled receptor (vasopressin 1 receptor, V1R) could also induce a significant *LMCD1* gene upregulation in response to its agonist stimulation (Figure 7.D). Next, we investigated the contribution of G protein-independent pathways, using β -arrestin biased AT1R agonist TRV120023 (TRV3). TRV3 stimulated cells did not increase *LMCD1* mRNA expression which indicates that the β -arrestin signaling pathway has no prominent role in the AngII-mediated *LMCD1* upregulation (Figure 7.C).

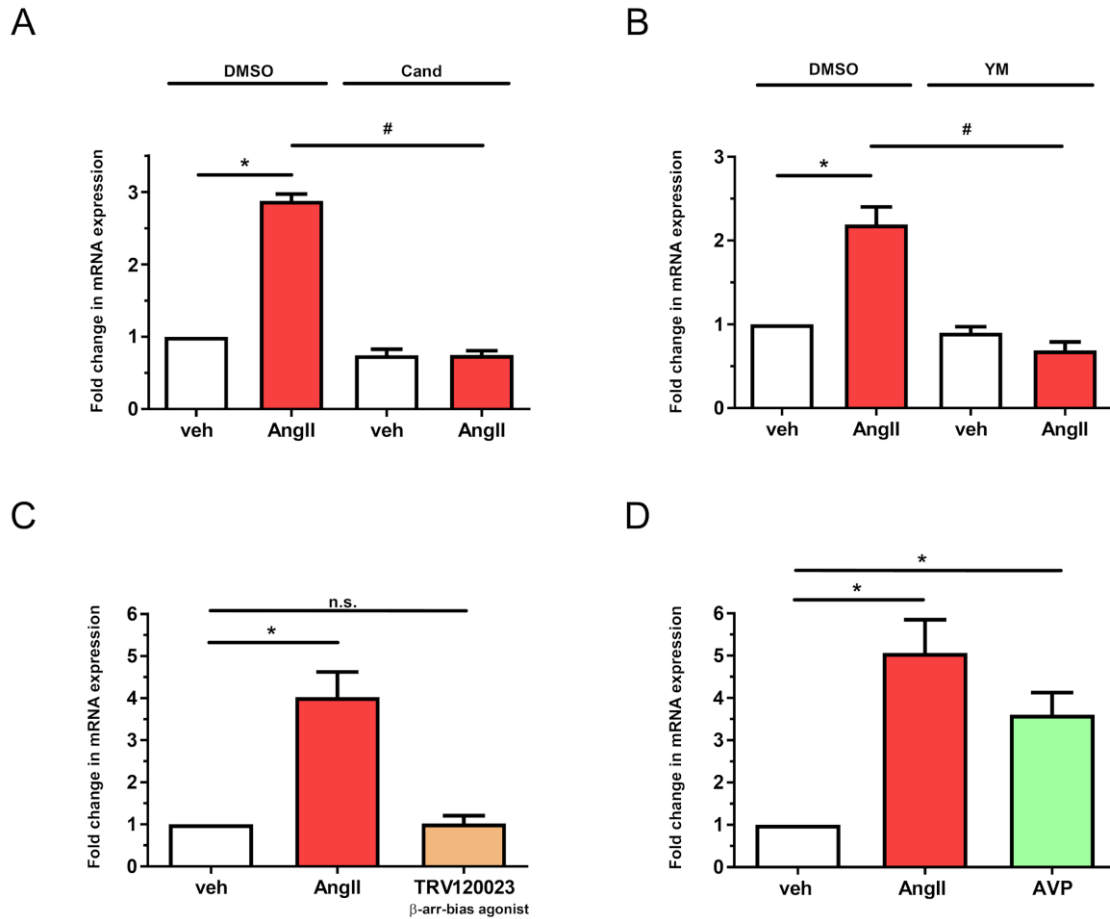


Figure 7. Role of AT1-R and Gq/11 signaling in AngII-mediated *LMCD1* expression. VSMCs were received overnight serum withdrawal before pharmacological inhibitor pretreatments and agonist treatments. mRNA levels were measured using quantitative real-time PCR, and measured results were normalized to the level of *GAPDH* housekeeping gene. (A) VSMCs were pretreated with 10 μ M Candesartan (Cand) or DMSO (control) for 30 minutes, followed by stimulation with vehicle (white columns) or 100nM AngII (red columns) for 2 hours ($n = 4$). Data are shown as values normalized to DMSO vehicle samples (mean \pm S.E.). (B) VSMCs were pretreated with 1 μ M YM-254890 (YM) or DMSO (control) for 30 min, then stimulated with vehicle (white columns) or 100 nM AngII (red columns) for 2 hours ($n = 6$). Data are shown as values normalized to DMSO/ vehicle samples (mean \pm S.E.). (C) VSMCs were incubated with vehicle (white column), 100 nM AngII (red column), or 3 μ M TRV120023 (β -arrestin-bias agonist, beige column) for 2 hours ($n = 3$). (D) VSMCs were stimulated with vehicle (white column), 100 nM AngII (red column), or 1 μ M AVP (green column) for 2 hours ($n = 5$). Mean values \pm SE are shown. Statistical significance was determined using multiple linear regression (A,B) or 1-way ANOVA (C,D), with $p < 0.05$ was considered to be statistically significant. Significance compared to vehicle stimulation is indicated by *; significance compared to DMSO-pretreated agonist-induced response is indicated by #; while n.s. indicates not statistically significant ($p > 0.05$).

4.2.4. Role of secondary messengers in the upregulation of *LMCD1*

$G_{q/11}$ proteins are able to activate phospholipase $C\beta$, which cleaves phosphatidylinositol-4,5-bisphosphate to IP_3 and DAG and. IP_3 induces the elevation of intracellular Ca^{2+} level, while DAG activates protein kinase C (PKC). We wanted to examine the role of calcium signal by pretreating cells with BAPTA-AM, a Ca^{2+} chelator. As shown in Figure 8.A, the elimination of calcium signal completely abolished the AngII-mediated *LMCD1* upregulation (Figure 8.A). Inhibition of Ca^{2+} /calmodulin dependent protein kinase II (CaMKII) with 50 μ M CK-59 also resulted in significant decrease in *LMCD1* expression decrease (Figure 8.B), which establishes the crucial role of calcium dependence of the AngII mediated *LMCD1* upregulation. As for the PKC pathway, pretreatment of the VSMCs with 1 μ M PKC inhibitor RO31-8425 caused a smaller, but not significant decrease in AngII provoked *LMCD1* upregulation (Figure 8.C). Performing inhibition of FAK and Pyk2, which are important pathways of MAPK cascade activation, using 1 μ M PF-562271 did not reduce AngII mediated *LMCD1* upregulation, which suggests, that these pathways have less importance in the examined process as well (Figure 8.D).

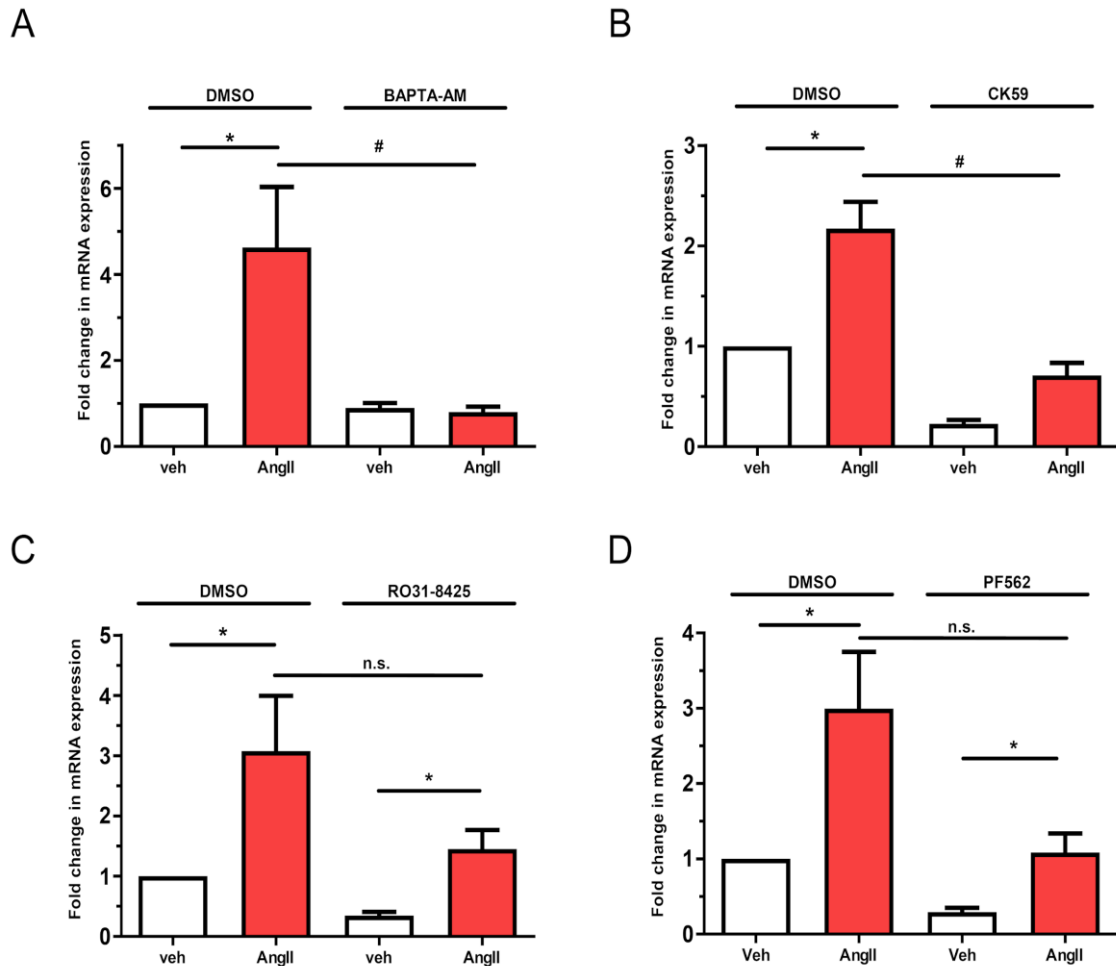


Figure 8. Investigation of calcium signaling and calcium-dependent kinases in AngII-mediated upregulation of *LMCD1* in vascular smooth muscle cells. Serum-depleted VSMCs were pretreated with either DMSO (control) or with one of the following inhibitors: (A) Ca^{2+} chelator 50 μM BAPTA-AM for 10 minutes, (B) 50 μM CamKII inhibitor CK59 for 30 minutes, (C) 1 μM PKC inhibitor RO31-8425 for 10 minutes, or (D) 1 μM PF-562271 (PF562) Pyk2 inhibitor for 30 minutes. After inhibitor pretreatment, cells were incubated with either vehicle (white columns) or 100 nM AngII (red columns) for 2 hours. mRNA was then isolated, then converted to cDNA, and *LMCD1* expression levels were measured by qRT-PCR and normalized to the *GAPDH* housekeeping gene. Data are shown as values normalized to DMSO/vehicle samples (mean \pm S.E.). Statistical significance was calculated using multiple linear regression, with $p < 0.05$ considered to be statistically significant. Significance compared to vehicle stimulation is indicated by *; significance compared to DMSO-pretreated agonist-induced response is indicated by #; while n.s. indicates not statistically significant ($p > 0.05$). Values represent three to five independent experiments ($n = 3-5$).

4.2.5. Role of MAPKs in AngII-mediated *LMCD1* upregulation

The activation of MAPKs have been proven to mediate various AngII-mediated gene expression changes. In order to identify which MAPK isoforms play an important role in the upregulation of *LMCD1*, we employed specific inhibitors. For these experiments, we performed pretreatments targeting different MAPK pathways: PD-98059 for MEK/ERK1/2, SB-202190 for p38 MAPK, and SP-600125 for JNK. Figure 9.A and 9.B demonstrates that the inhibition of the MEK/ERK1/2 and the JNK pathways did not significantly reduce the AngII-mediated increase of *LMCD1* expression. In contrast, the pretreatment with 50 μ M SB-202190 completely inhibited the AngII-induced response (Figure 9.C). As ROS production is a common activator in VSMCs of MAPK pathways that is an important mechanism of vascular remodeling in pathological conditions, we also investigated the importance of ROS production in AngII mediated *LMCD1* upregulation by inhibiting NADPH oxidase activity using diphenyleneiodonium (DPI). 5 μ M DPI pretreatment did not reduce the *LMCD1* upregulation at all in response to AngII stimulation (Figure 9.D), and therefore suggests that ROS production does not play a role in the examined process.

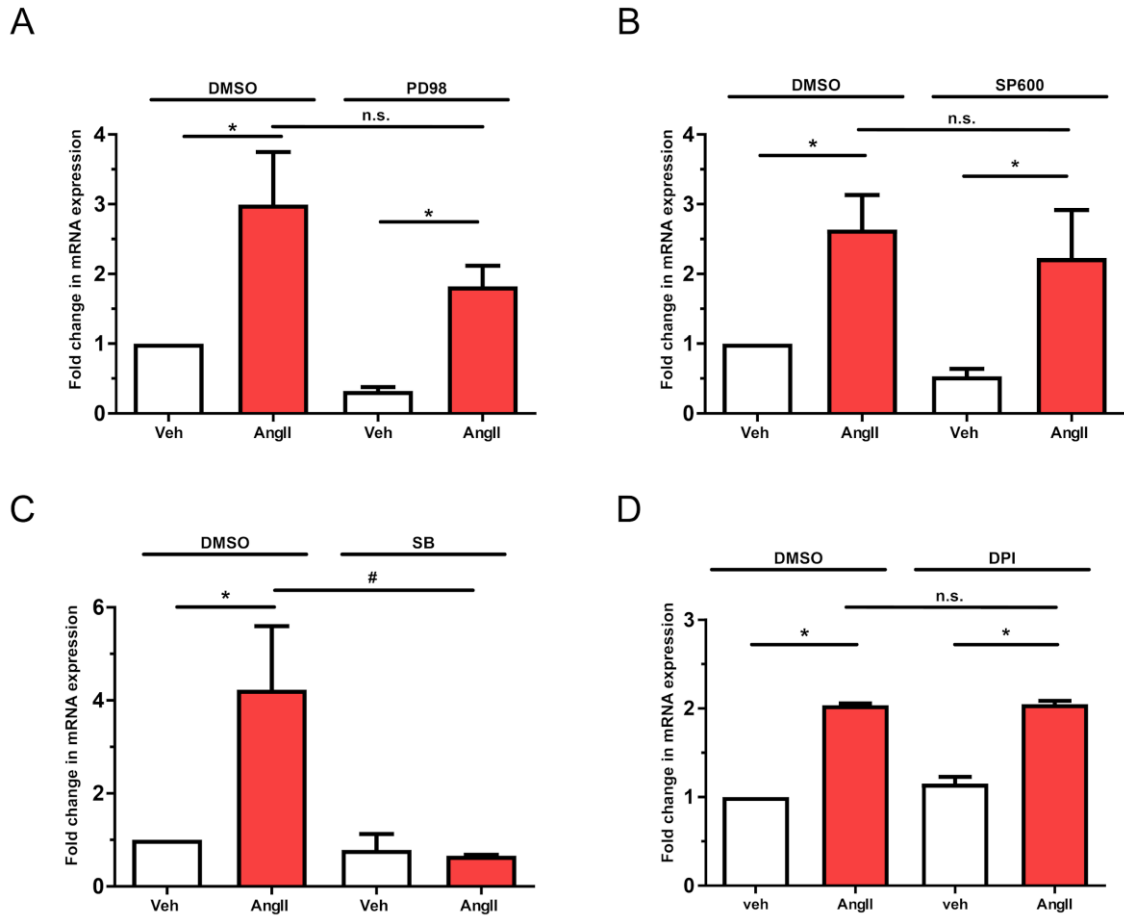


Figure 9. Role of different MAPKs in AngII mediated *LMCD1* upregulation. After overnight of serum withdrawal, VSMCs were pretreated for 30 minutes with 20 μ M MEK inhibitor PD-98059 (PD98) (A), 25 μ M of JNK inhibitor SP-600125 (SP600) (B) or 50 μ M of p38 MAPK inhibitor SB-202190 (SB) (C) and additionally with 50 μ M NADPH oxidase inhibitor DPI (D), whereas the control cells were pretreated for 30 minutes with DMSO. Following pretreatments, the cells were exposed to 2 hour 100 nM AngII stimulation (red columns), or treated with vehicle (veh) (white columns). After the treatments, mRNA was isolated from the VSMCs, then transcribed to cDNA samples. Expression levels of *LMCD1* were measured with real-time quantitative PCR. Standardization was made against house-keeping gene *GAPDH*. Data are shown as values normalized to DMSO/vehicle samples (mean \pm S.E.). Statistical significance was calculated using multiple linear regression, with $p < 0.05$ considered to be statistically significant. Significance compared to vehicle stimulation is indicated by *; significance compared to DMSO-pretreated agonist-induced response is indicated by #; while n.s. indicates not statistically significant ($p > 0.05$). Values represent three to five independent experiments ($n = 3-5$).

4.3. Investigation of functional role of LMCD1 in vascular smooth muscle cells

4.3.1. Effect of LMCD1 on cellular proliferation and migration

It has been reported that LMCD1 increases cellular proliferation and hypertrophy in various cell types (53,55–57). We set out to investigate whether it has similar roles in vascular smooth muscle. Therefore, we overexpressed LMCD1 by the transfection of an LMCD1 overexpressing pcDNA plasmid construct. We used A7r5 cells for these experiments, because primary VSMCs cannot be transfected effectively. In order to compare cellular proliferation in cells overexpressing LMCD1 to non-overexpressing control (transfected with empty pcDNA plasmids) cells, ³H-leucine incorporation assay was used. 24 hours after the transfection, cells were treated with ³H-labeled leucine containing medium for an additional 24 hours, after which scintillation counts of the samples were measured. Across four independent experiments, we measured an approximately 15% increase in ³H-leucine incorporation in LMCD1 overexpressing cells compared to the control group (Figure 10.B), even though the transfection efficiency was approximately 15-20% (Figure 10.A).

To determine the effect of LMCD1 overexpression on A7R5 cells' migration, wound-healing assay was performed. 24 hours after transfection, the monolayer of A7R5 cells was scraped with a sterile 200µl pipette tip, then wounds were photographed with a microscope at 5x loop. Medium was exchanged to serum reduced (2% FBS containing) DMEM for 48 hours, to prevent errors given by increased cell growth of the LMCD1 overexpressing cells. After 2 days of serum reduction the wounds were photographed again, then wound areas were measured. At Figure 10.C we can observe a more spectacular decrease of the wound area after 48 hours in case of LMCD1 overexpressing cells compared to the control. Five independent experiments showed that in case of control cells, the wound area only reduced by 35% in 48 hours, while in LMCD1 overexpressing groups wound areas decreased by approximately 50% in 48 hours (Figure 10.C and D).

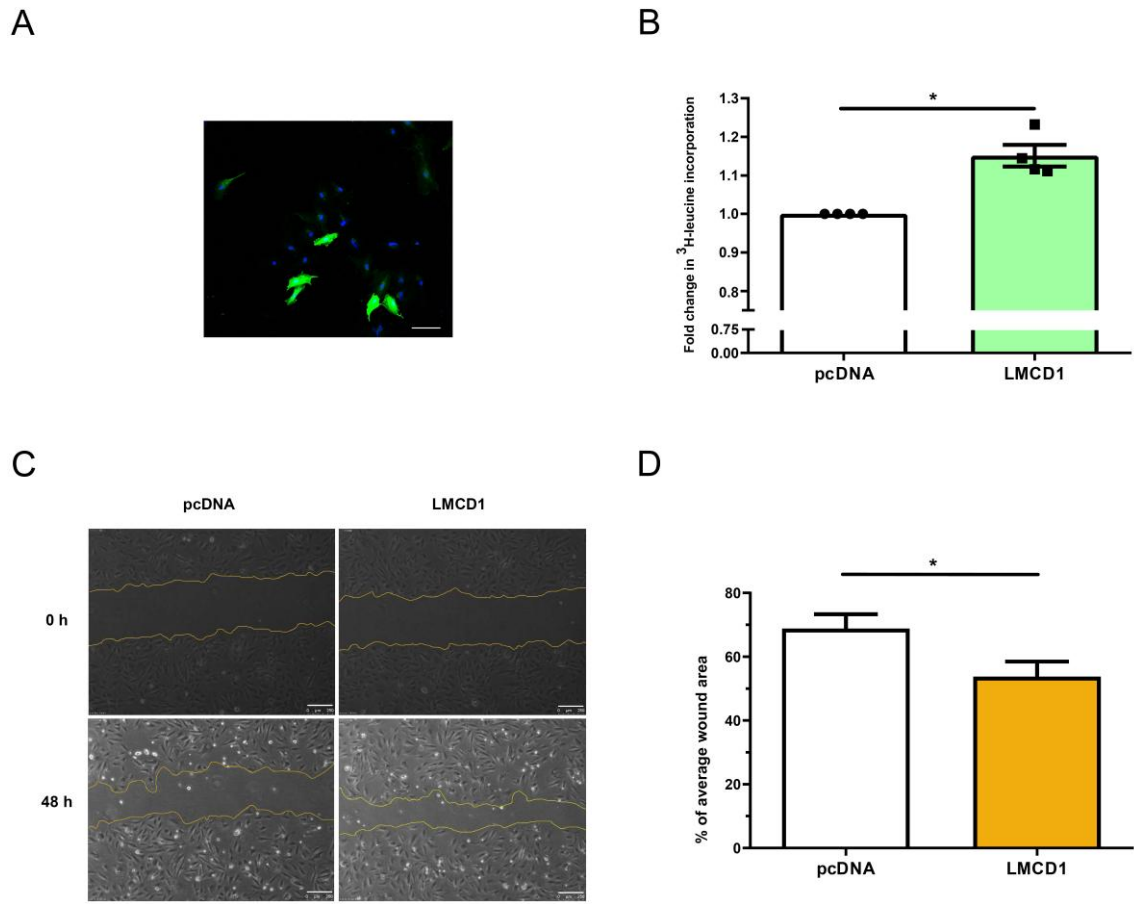


Figure 10. Effect of LMCD1 overexpression on cellular proliferation and migration. (A) A7r5 cells were transfected with LMCD1-overexpressing plasmids, fixed with PFA and stained with anti-LMCD1 primary antibody, then AlexaFluor488-labeled secondary antibody (green). The nuclei were stained with To-Pro reagent (blue). Immunofluorescent images were taken using a Zeiss LSM710 confocal laser-scanning microscope. Scale bar represents 100 μm . (B) To measure cellular proliferation, A7r5 cells were transfected with pcDNA-LMCD1 (green column) or non-LMCD1 overexpressing pcDNA plasmids (control) (white column). 24 hours after transfection, cells were incubated with ^3H -leucine containing medium for 24 hours, then samples were collected to scintillation measurement. Scintillation counts were measured for 2 minutes. Fold change in ^3H -leucine incorporation is shown. Mean values \pm S.E. are shown ($n=4$). Significance was determined with paired t-test ($p < 0.05$). (C-D). For wound-healing assay, A7R5 cells were transfected with LMCD1 expressing pcDNA-LMCD1 plasmids (yellow column), while control cells were transfected with pcDNA-Empty plasmids (white column). 24 hours after the transfection, wounds were scraped in the layer of cells with a 200 μl pipette tip. Images were taken at 5x loop. 48 hours later, wounds were photographed again at the same positions. Areas of wounds were measured. Percentage of original wound areas are shown. Significance was determined with paired t-test ($p < 0.05$). ($n=4$).

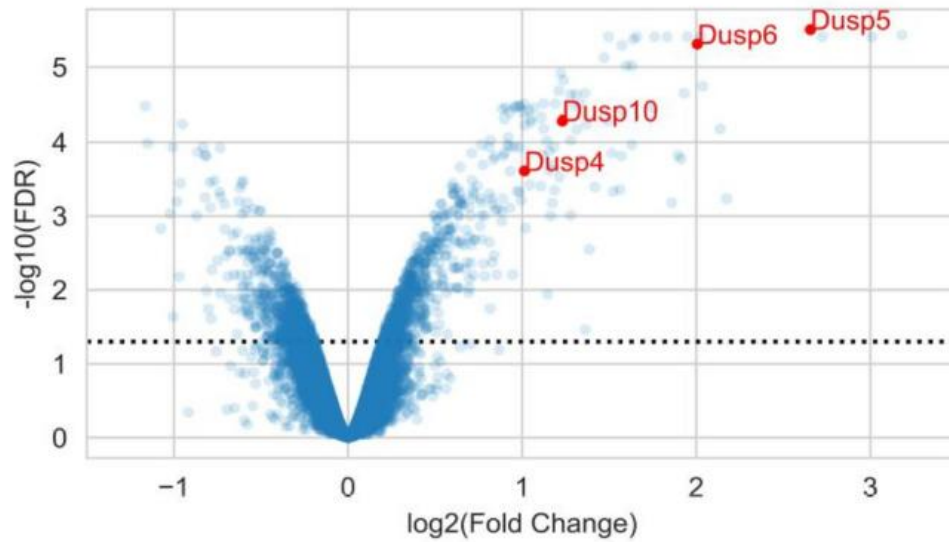
4.4. Importance of EGFR transactivation in AngII mediated gene expression changes

4.4.1. Identification of additional gene targets

Performing Affymetrix Gene Chip Rat gene 1.0 ST array on primary rat VSMCs, treated for 2 hours with 100nM AngII or vehicle, as control, we identified numerous genes that show up- or downregulation to AngII treatment. Using differential expression analysis between AngII and vehicle treated samples, 74 genes were identified to become upregulated for AngII stimuli, including *LMCD1*, I discussed earlier in this thesis (Figure 4.). Among the 74 genes, four different dual specificity phosphatase genes, namely *DUSP4*, *DUSP5*, *DUSP6* and *DUSP10* showed significant AngII induced upregulation (Figure 11.A).

For pathway activity analysis, we performed PROGENy tool to characterize a more unbiased analysis of gene expression changes, provoked by AngII treatment. Figure 11.B shows 14 identified upstream pathways that play a significant role in the case of the observed gene expression changes. According to the z-scores of pathway activities, AngII treatment induced EGFR and MAPK pathway activity at the most significant level. In our further experiments, we are focusing on the importance of the transactivation of the EGFR pathway in the context of AngII mediated long-term effects in primary VSMCs.

A



B

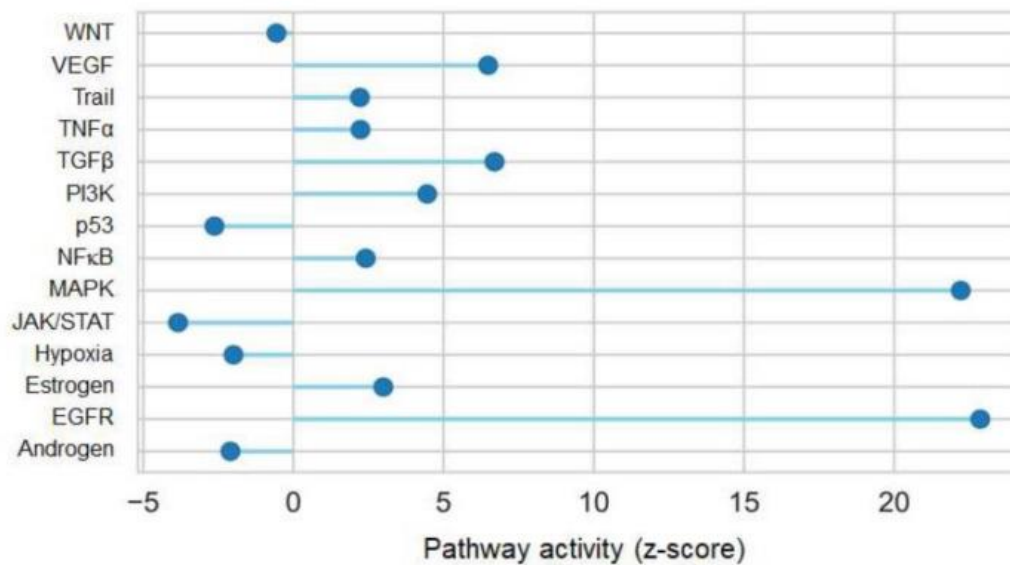


Figure 11. Gene expression changes of DUSP isoforms in response to AngII stimulation in VSMCs. The volcano plot illustrates the differential expression analysis (DE) of the gene expression changes provoked by 2 hours of 100nM AngII treatment in VSMCs, the experiment was performed on triplet samples (A). On the x-axis, log₂ fold change is shown, while y-axis performs $-\log_{10}$ false discovery rate (FDR), based on Benjamin-Hochberg correction of p-values. Significance threshold (FDR>0,05) is labeled with the dotted horizontal line. Selected DUSP isoforms are highlighted with red color. Figure B illustrates the PROGENy pathway analysis of the AngII mediated gene expression signature. On the x-axis, PROGENy pathways are labeled, while on the y-axis, activity scores are shown, calculated using a multivariate linear model.

4.4.2. Lentiviral silencing of *EGFR*

In order to examine the importance of AT1R-mediated EGFR transactivation, we aimed to silence *EGFR* gene expression by the help of specific short hairpin RNAs (shRNA). The shRNAs can interfere with a complementary mRNA causing its degradation and thereby preventing its translation, by preventing the expression of the protein encoded by that mRNA. To deliver the *EGFR*-specific shRNA sequences into primary VSMCs, lentiviral constructs were used. At the beginning, we created two different shRNA constructs. To determine their effectiveness in *EGFR* silencing, we infected cells with both lentiviral constructs alongside a control group, infected with an ‘empty’ lentiviral construct that did not encode *EGFR*-specific shRNA sequences. Cells were harvested for real-time quantitative PCR measurement 48 hours after the infection to examine the shRNA caused decrease in *EGFR* gene expression and also to Western blot assay to observe the reduction in the activity of EGFR protein (Figure 12.A). As shown in Figure 12.A, both shRNA#1 and shRNA#2 constructs significantly reduced the mRNA level of *EGFR*, but the shRNA#2 construct seemed to be more effective. At the protein level, the amount of activated EGFR was also effectively reduced by both constructs, though the shRNA#2 construct again demonstrated a more pronounced effect (Figure 12.B). Based on these results, we selected the shRNA#2 construct for our subsequent experiments.

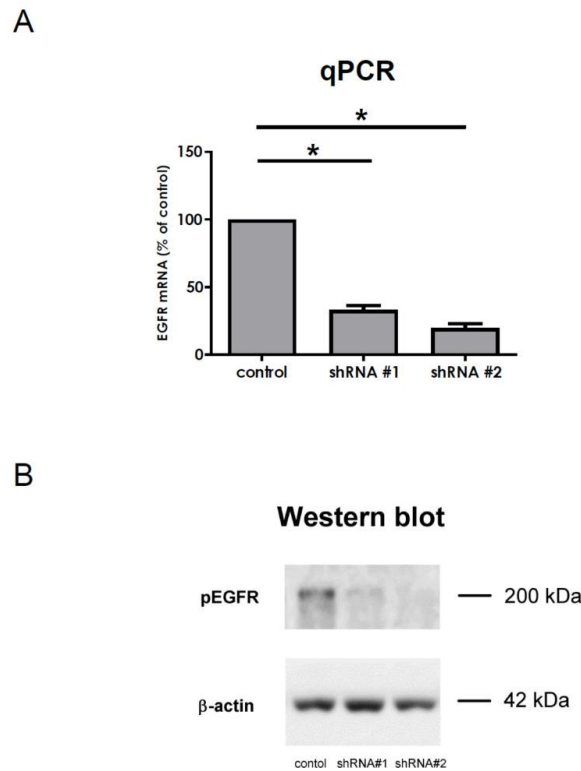


Figure 12. Lentiviral silencing of *EGFR*. Lentiviral infection was performed on VSMCs to silence *EGFR* with shRNAs. For this purpose, two different lentiviral constructs were used (shRNA #1 and shRNA #2) beside a control group infected with empty lentiviral particles (control). 48 hours after the infection, samples were taken for gene expression measurement (A). mRNA was isolated from cells, then samples were converted to cDNA. Gene expression of *EGFR* was measured via normalization to the *GAPDH* housekeeping gene. Percentage of original *EGFR* expression is shown. Mean values \pm SE are shown ($n = 3$). Significance was calculated with a one-way ANOVA test ($p < 0.05$). For protein expression measurement, samples were assessed in western blot assay (B), where anti- β -actin staining was used as a loading control. The western blots shown are representative of three independent experiments ($n = 3$).

4.4.3. Comparing pharmacological inhibition and genetic silencing of EGFR

Pharmacological inhibitors often have off-target target molecules, which can lead to misleading interpretations of experimental results. We aimed to examine the differences between the effect of pharmacological inhibitors and genetic silencing, we compared the effects of two specific EGFR inhibitors, AG1478 and gefitinib, to the effects of shRNA mediated *EGFR* silencing. To this end, the expression of *DUSP* genes, significantly upregulated by AngII, was investigated first by pharmacological inhibition of EGFR and then by genetic silencing of the *EGFR* gene with shRNA. For this purpose,

we examined the AngII-mediated expression of three different DUSP isoforms, *DUSP5*, *DUSP6* and *DUSP10*, that are significantly upregulated in response to AngII stimuli in VSMCs, according to the results of Affymetrix gene chip assay (Figure 11.A) and the changes in their upregulation affected by pharmacological inhibition of EGFR and shRNA mediated silencing of *EGFR* was assessed.

4.4.3.1. Effect of pharmacological inhibition of EGFR transactivation on AngII-mediated upregulation of *DUSP* isoforms

Based on the result of pathway analysis, AT1R-induced EGFR transactivation seemed to play a key role in AngII mediated gene expression changes (Figure 11.B). First, we wanted to investigate the effects of EGFR pharmacological inhibition on the AngII-mediated upregulation of *DUSP5*, *DUSP6* and *DUSP10* genes (Figure 13.A-C). All three genes were significantly upregulated by AngII, while *DUSP6* also showed a significant upregulation in response to EGF stimulation on its own. When the activity of EGFR was inhibited by 1 μ M AG1478 or 2.5 μ M gefitinib, we observed a massive reduction in the AngII-mediated gene expression response in all the three *DUSP* genes. These data could suggest that the AT1R-mediated EGFR transactivation might play a crucial role in the AngII-mediated upregulation of the examined genes. However, inhibition of matrix-metalloproteinase, which is an essential step in AngII-induced EGFR transactivation, showed a significant effect only in the case of *DUSP5* (Figure 13.D), but was insignificant in case of *DUSP6* (Figure 13.E) and *DUSP10* (Figure 13.F). These results raise questions whether EGFR transactivation by AT1R is really that important in AngII-mediated gene expression changes as it was previously thought.

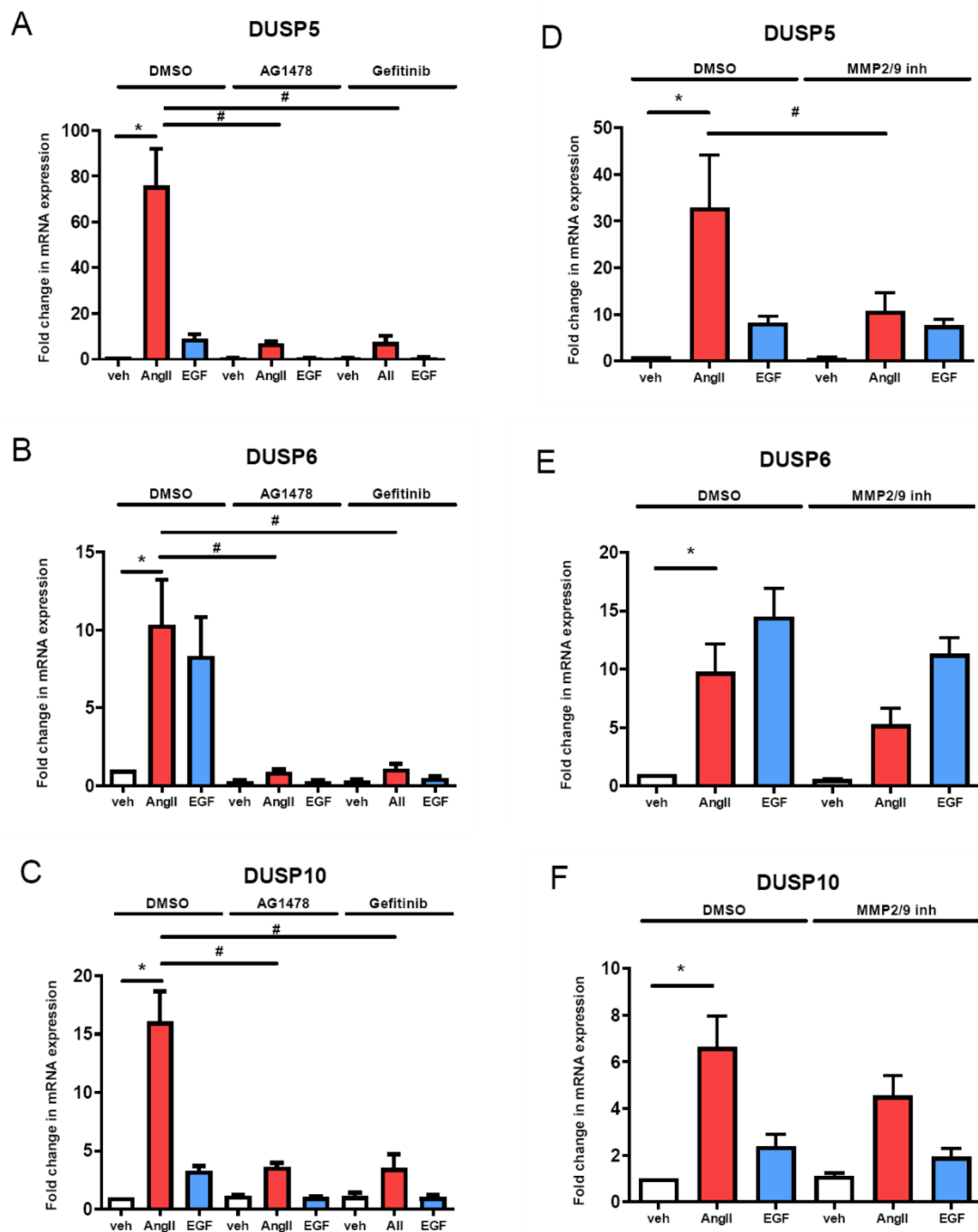


Figure 13. Effect of pharmacological inhibition of EGFR on the AngII-mediated upregulation of DUSP isoforms. VSMCs were serum-starved overnight, then pretreated with 1 μ M AG1478 or 2.5 μ M gefitinib (A-C), 1 μ M MMP2/MMP9 inhibitor (MMP2/9 inh) (D-F) or DMSO, as control for half an hour. After pretreatment, cells were stimulated with 100 nM AngII (red columns), or 500 ng/ μ l EGF (blue columns), or vehicle (white columns), as control for 2 hours. From the collected samples, mRNA was extracted, then converted to cDNA. Expression levels of *DUSP5* (A and D), *DUSP6* (B and E) and *DUSP10* (C and F) were measured with real-time quantitative PCR. Standardization was measured via normalization to the house-keeping gene *GAPDH*. Normalized values are

shown to the DMSO/vehicle treated samples. Significance was determined with multiple linear regression analysis. $p < 0.05$ was considered as statistically significant. *: statistically significant from vehicle stimulation. #: statistically significant from DMSO-pretreated agonist-induced response. ($n = 3-6$).

4.4.3.2. Effect of shRNA mediated silencing of *EGFR* on AngII-induced upregulation of DUSP isoforms

The next step was the investigation, how the shRNA-mediated silencing of *EGFR* affects the upregulation of DUSP isoforms in response to AngII stimuli. As shown in Figure 14, the silencing of *EGFR* had much less effect on AngII-mediated upregulation of the examined DUSP isoforms. Among the three DUSP isoforms, we observed a statistically significant decrease only in case of *DUSP5* expression in AngII-induced upregulation after shRNA-mediated *EGFR* silencing (Figure 14.A). This limited impact is not attributable to ineffective lentiviral transduction, as upregulation of *DUSP6* in response to EGF was completely abolished in cells infected with shEGFR constructs, confirming successful silencing. These findings cast doubt on the previously assumed central role of AT1R-mediated EGFR transactivation in the upregulation of the three DUSP isoforms.

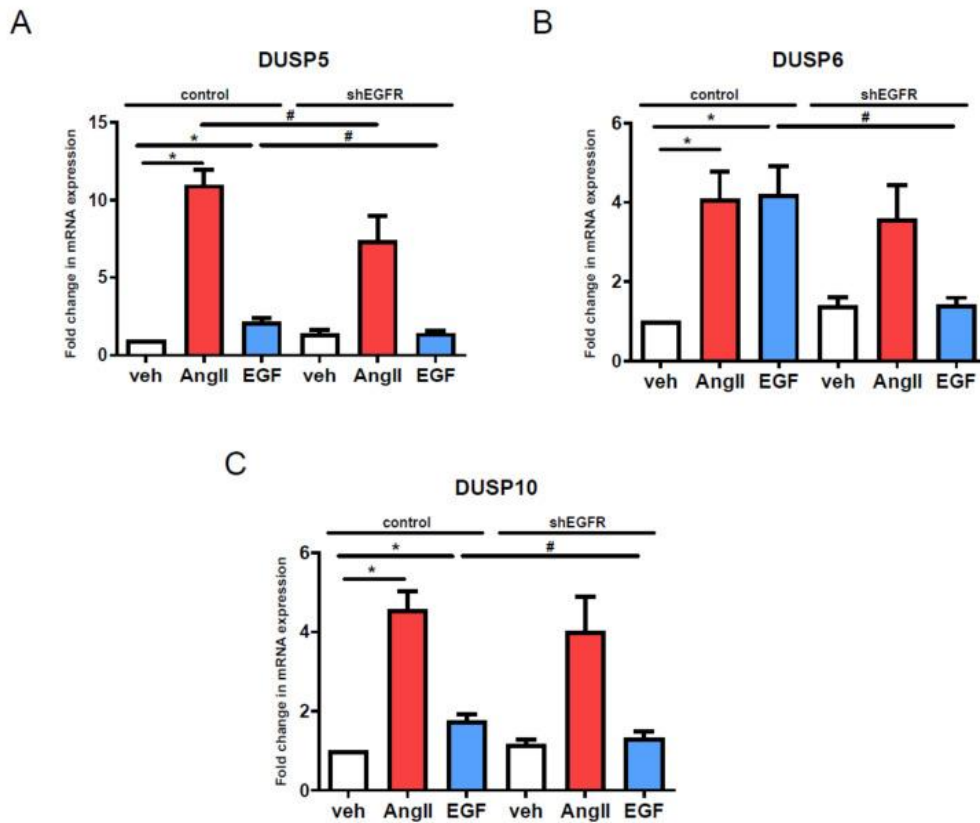


Figure 14. Effect of shRNA-mediated silencing of *EGFR* on the AngII-induced upregulation of DUSP isoforms. VSMCs were infected with *EGFR* silencing shEGFR lentiviruses, while control cells were infected with empty lentiviral particles (control). One day after the infection, cells were exposed to overnight serum depletion. Next day, VSMCs were treated with 100 nM AngII (red columns), or 500 ng/ μ l EGF (blue columns) or vehicle (white columns), as control for 2 hours. Thereafter, mRNA was isolated from cellular samples and was converted to cDNA. Gene expression levels of *DUSP5* (A), *DUSP6* (B) and *DUSP10* (C) were measured with real-time quantitative PCR. Standardization was made against housekeeping gene *GAPDH*. Normalized values are shown to the control/vehicle samples. Mean values \pm S.E. are shown. Significance was determined with multiple linear regression. $p < 0.05$ was considered as statistically significant. *: Statistically significant from vehicle stimulation. #: Statistically significant from control virus-infected agonist-induced response. ($n = 4$).

4.4.4. Potential pathways beside EGFR-transactivation

It is possible that beside EGFR, other tyrosine kinases can play a role in the AngII-mediated upregulation of the examined genes. Additionally, it is important to consider that pharmacological inhibitors often have off-target molecules, so it is conceivable that AG1478 and gefitinib inhibited other tyrosine kinases beside EGFR and that is the reason,

how they were able to abolish the AngII-mediated upregulation of the examined genes (Figure 13.A-C), while *EGFR* silencing alone did not exert significant impact (except in case of *DUSP5*) (Figure 14.). Here, we pretreated VSMCs before agonist stimulation with 1 μ M dasatinib, a broad-spectrum tyrosine kinase inhibitor. Dasatinib is usually used in the treatment of chronic myeloid leukemia, a potent inhibitor of BCR/ABL and Src kinase family, but can also target c-kit, ephrin receptor or PDGF β receptor (61,62). As shown in Figure 15, dasatinib pretreatment significantly decreased the AngII-mediated upregulation of all the three *DUSP* isoforms. These results suggest that in addition to EGFR, other dasatinib-sensitive tyrosine kinases are likely responsible for the gene expression changes after AngII stimulation.

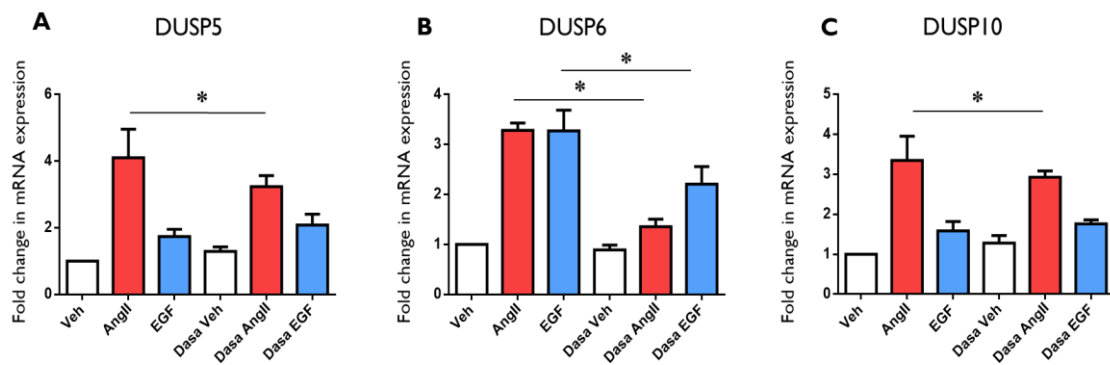


Figure 15. Effect of dasatinib pretreatment on AngII- and EGF-mediated upregulation of DUSP isoforms. VSMCs received overnight serum depletion, then were incubated with 1 μ M dasatinib or DMSO for 30 minutes. Pretreated cells were stimulated with 100 nM AngII, 50 μ g/ml EGF or vehicle for 2 hours. Thereafter, RNA was isolated and converted to cDNA samples. The mRNA levels of *DUSP5* (A), *DUSP6* (B) and *DUSP10* (C) were measured with real-time qPCR. Standardization was made against house-keeping gene *GAPDH*. Data normalized to the vehicle/DMSO samples are shown. Mean values \pm S.E. are shown. Significance was determined with multiple linear regression. $p < 0.05$ was considered as statistically significant. *: statistically significant from vehicle stimulation. #: statistically significant from DMSO-pretreated agonist-induced response. ($n = 3-4$). Unpublished data.

5. Discussion

The exaggerated effects of AngII have been shown to be major contributors in the formation of vascular remodeling, that plays a key role in the pathogenesis of numerous common and severe diseases, including atherosclerosis, hypertension, stroke, and myocardial infarction (59,60). To develop effective prevention and treatment methods against these widespread diseases, it is crucial to understand the molecular mechanisms mediated by AngII, that lead to these pathological conditions. During my PhD work, I mainly focused on the gene expression changes mediated by AngII in vascular smooth muscle cells, including signal transduction pathways and certain specific genes that might contribute to the vascular remodeling processes.

Using an Affymetrix gene chip array, we identified numerous genes that are significantly up- or downregulated in primary rat VSMCs to AngII stimulation. Additionally, pathway analysis with PROGENy tool was performed to identify the most important signaling pathways that contribute to AngII mediated gene expression changes (Figures 4 and 11). In particular, the results of these examinations served as starting points for the research of my PhD work. Among the significantly upregulated genes, *LMCD1* (also known as *Dyxin*) seemed to be quite interesting, as it was described to play a role in different proliferative cellular processes, even though there were just few papers published concerning its function and expression. One of the goals of my research was to investigate how this gene is upregulated by AngII and to explore the most important effects of LMCD1 protein in the physiology VSMCs.

First, we investigated the kinetic changes over time of *LMCD1* mRNA and protein expression, since the determination of the time point of the maximal expression was essential for the design of the subsequent experiments. As shown in the results, it was observed that *LMCD1* mRNA expression peaked between 1 and 3 hours after AngII treatment (Figure 5.A), while protein expression reached its maximum 24 hours after VSMCs were stimulated with AngII (Figure 5.B and 5.C). It must be mentioned that we performed experiments measuring the expression of other genes parallel, that were also upregulated by AngII, such as *DUSP5*, *DUSP6* and *DUSP10* genes. The 2-hour AngII stimulation seemed to be optimal in case of all the four genes (Figure 5.A), so the subsequent experiments were performed with 2-hour AngII stimulations.

Interestingly, the immunofluorescent pictures (Figure 6.C) revealed that *LMCD1* was not only localized in the nucleus, as it could be expected from a transcription cofactor, but it was also observed in cellular compartments around the nucleus. Based on the morphology of the fluorescent signal, we hypothesized that *LMCD1* was accumulated in the Golgi-apparatus. Moreover, the signal there became stronger from 4 to 24 hours after the AngII stimulation. To identify the cellular compartment, where *LMCD1* showed such significant accumulation, immunostaining with cis- and trans-Golgi markers were performed. As Figure 6. demonstrates, *LMCD1* showed colocalization with trans- and cis-Golgi-apparatus. Interestingly, in other cell types, the localization of *LMCD1* was mainly described in the nucleus or the cytosol (53,61,62) , and no data was found about *LMCD1* location in the Golgi apparatus. This observation raises interesting questions, whether *LMCD1* may have Golgi-related functions or whether this localization is specific to VSMCs. These questions were not addressed in this thesis, but they can serve as interesting topics for future investigations.

Another key objective of my PhD work was the investigation of signaling pathways leading to the AngII-mediated upregulation of *LMCD1* in VSMCs. AngII exerts most of its cardiovascular effects through AT1R activation, with $G_{q/11}$ protein coupling. However, AngII pleiotropic signaling pathways, including G protein-dependent and independent pathways, and AngII has certain affinity to AT2R, as well (27,66). Performing pharmacological inhibition of AT1R and $G_{q/11}$ protein showed that both are essential for AngII to increase the expression of *LMCD1*. Moreover, stimulating VSMCs with β -arrestin-biased agonist TRV120023 produced no significant elevation of *LMCD1* mRNA level, supporting the conclusion that AngII upregulates *LMCD1* through AT1R and $G_{q/11}$ protein activation (Figure 7.A-C). In VSMCs, it was described earlier that thrombin upregulates *LMCD1* through $G_{q/11}$ activation (57) and stimulating VSMCs with AVP, which hormone also exerts most of its effects through $G_{q/11}$ protein activation also increased the expression of *LMCD1* (Figure 7.D).

It is widely established that $G_{q/11}$ activation leads to Ca^{2+} release from the ER to the cytosol through IP_3 production and to PKC activation by DAG - secondary messengers that play key roles in various signaling pathways initiated by AT1R activation (2). Chelation of Ca^{2+} completely abolished AngII-mediated *LMCD1* upregulation (Figure 8.A), while inhibition of PKC had no significant effect.

MAPK cascades are well-known effectors of AT1R signal transduction that mediate gene expression changes (63,64). Results of PROGENy pathway analysis also confirmed that the MAPK pathway is remarkably active in response to AngII stimulation in primary VSMCs (Figure 11.B). We wanted to identify which MAPK isoform plays a prominent role in the AngII-mediated *LMCD1* upregulation. Pharmacological inhibition of p38 MAPK completely prevented the AngII-mediated increase of *LMCD1* expression, while the inhibition of ERK1/2 and JNK pathways had no significant effect. These findings are consistent with our group's earlier studies on other AngII-responsive genes (65). In fact, p38 pathway is often activated by environmental stress and inflammatory cytokines and was reported to play a prominent role in the pathogenesis of several cardiovascular diseases (36,66,67). *LMCD1* overexpression significantly increased cellular proliferation and migration in VSMCs (Figure 10.) which are essential steps of pathological vascular remodeling. Our data suggests that AngII-mediated *LMCD1* upregulation via p38 pathway activation might play a role in the vascular remodeling process and in the pathogenesis of cardiovascular diseases, related to the excessive activity of RAAS.

Beyond the MAPK cascade activation, the results of PROGENy pathway analysis revealed that EGFR pathway activation is particularly strong in response to AngII stimulation in VSMCs (Figure 11.B). EGFR transactivation by AT1R is well known to mediate proliferative effects of AngII (4), via activation of Src kinases, MAPK cascades, and potentiating calcium signal (68,69). We examined the importance of EGFR transactivation in case of three *DUSP* isoforms that are significantly upregulated in VSMCs in response to AngII stimulation (Figure 11.A). *DUSP* proteins are important regulators of the MAPK cascades that not only inhibit the activity of MAP kinases by dephosphorylation on their tyrosine and threonine residues, but they can also control the spatiotemporal dynamics of the different MAPKs (70,71). Our results show that EGFR specific pharmacological inhibitors effectively decreased AngII-induced upregulation of all the three examined *DUSP* isoforms (Figure 13.). In case of *DUSP6*, stimulation of the EGF receptor by its agonist alone could robustly elevate the gene's expression level (Figure 14.B), while in the case of *DUSP5* and *DUSP10*, the effect of EGF was significant, but less spectacular (Figure 14. A and C). On Figure 13. we could observe a massive decrease in the AngII mediated upregulation in the case of all the three *DUSP*

isoforms. These data suggested that EGFR transactivation has a prominent role in case of the AngII-mediated upregulation of these genes, but it must be highlighted that pharmacological inhibitors often have off-target molecules, whose inhibition leads to misleading conclusions. Based on literature data, the AT1R-mediated transactivation of EGFR occurs via matrix-metalloproteinase activation (4). Interestingly only *DUSP5* showed a significant decrease in AngII-induced upregulation using an MMP2/MMP9 inhibitor (Figure 13.D), but in case of *DUSP6* and *DUSP10* its effect was statistically insignificant (Figure 13.E and F). These results confirm the proposition that the importance of EGFR transactivation must be evaluated very carefully.

In order to further clarify EGFR's role, we designed lentiviral constructs expressing EGFR-specific shRNAs to reach more specific, genetic silencing of *EGFR* (Figure 12.). With the two designed constructs, significant downregulation of *EGFR* mRNA expression and EGFR activity was reached, and in case of shEGFR#2 a slightly greater efficacy can be observed (Figure 12.), therefore the shRNA#2 construct was utilized in the subsequent experiments. Infecting cells with *EGFR* specific shRNA expressing lentiviral construct produced similar results as the MMP2/MMP9 inhibition. The genetic silencing of *EGFR* resulted a significant, but not as massive effect as AG1478 or gefitinib (Figure 13.A) on AngII-mediated upregulation of *DUSP5* (Figure 14.A), but did not significantly affect the *DUSP6* and *DUSP10* upregulation (Figure 14.B and 14.C). These results suggest that the AT1R-mediated EGFR transactivation has a significant role in case of *DUSP5* but is not a central mediator of AngII-induced gene expression for all three *DUSPs*.

The results of my PhD work obviously raise the questions if the EGFR transactivation is not the primary mechanism, then what other pathways play key roles in the AngII-mediated gene expression changes. To address this question, we pretreated VSMCs with various tyrosine-kinase inhibitors. Among those, dasatinib, a clinically used inhibitor of BCR/Abl and Src kinase family (72), provided promising results (Figure 15). Half an hour of 1 μ M dasatinib pretreatment on serum-starved VSMCs caused significant inhibition of AngII-mediated upregulation of all the three examined *DUSP* isoforms. In contrast, experiments done with imatinib pretreatment, a more specific inhibitor of BCR/Abl with limited effect on Src kinase activity (73) did not significantly inhibit the AngII-induced upregulatory effects (Figure 15.A-C).

The identification of the specific tyrosine-kinase or kinases that play a role in the examined process and also the investigation of their EGFR transactivation independent activation are key directions for future research. One of the most important future plans of our research group is to investigate these mechanisms further, and also to investigate the physiological roles of DUSP5, DUSP6 and DUSP10 in vascular smooth muscle cells, as well as their contribution to the long term effects of AngII, both *in vitro* and *in vivo*.

6. Conclusions

1. *LMCD1* is significantly upregulated by AngII in vascular smooth muscle cells. Its mRNA level peaks 1 to 3 hours after AngII stimulation, while the LMCD1 protein level reaches its maximum approximately 24 hours after AngII treatment.
2. In VSMCs, LMCD1 is mainly localized in the nucleus and shows significant accumulation in the Golgi apparatus after AngII stimulation.
3. AngII induces *LMCD1* upregulation activating AT1R, via G_{q/11} induced calcium signal and p38 MAPK activation.
4. LMCD1 overexpression leads to increased proliferation and migration in vascular smooth muscle cells.
5. MAPK cascade activation and EGFR transactivation seems to play crucial roles in AngII-induced gene expression changes in VSMCs.
6. Genetic silencing of *EGFR* is significantly less effective in AngII-mediated upregulation of certain genes compared to pharmacological inhibition.
7. It is possible that, in addition to EGFR, other tyrosine kinases, such as Src kinase family play key roles in AngII-mediated gene expression changes.

7. Summary

During my PhD work, my research mainly focused on the AngII provoked long term effects in the vascular smooth muscle cells.

Using Affymetrix gene-chip assay, we identified numerous genes, up- or downregulated in VSMCs to AngII stimuli. Firstly, we focused on *LMCD1*, the gene of a LIM-protein, basically regulating proliferative cellular functions as a transcriptional co-factor. We investigated the main signal transduction pathways that lead to *LMCD1* upregulation in VSMCs to AngII treatment. Furthermore, we described the effects of *LMCD1* protein overexpression on cellular proliferation and migration.

Due to the results of PROGENy pathway analysis, we evaluated the importance of AT1R dependent EGFR transactivation in VSMCs. We evaluated the importance of AT1R activation related EGFR transactivation in the case of the genes of three different dual specificity phosphatase isoforms, which were proved to be significantly upregulated by AngII in VSMCs. Our findings demonstrate that genetic silencing of *EGFR* did not cause such a spectacular reduction of AngII induced upregulation in the case of *DUSP5*, *DUSP6* and *DUSP10* genes, than we could measure using pharmacological inhibition of EGFR protein. Since pharmacological inhibitors often inhibit off-target proteins too, it is possible that there are other tyrosine-kinases that play an important role in the AngII-mediated upregulation of the three examined genes. Based on our yet unpublished data, we found proof that dasatinib sensitive tyrosine-kinases, like Src family kinases, might be responsible in this process, but the examination and description of the exact pathways leading to AngII mediated upregulation of *DUSP5*, *DUSP6* and *DUSP10* genes will have to be the subject of our future research.

8. References

1. Williams B. Angiotensin II and the pathophysiology of cardiovascular remodeling. *Am J Cardiol.* 2001 Apr 19;87(8):10–7.
2. Forrester SJ, Booz GW, Sigmund CD, Coffman TM, Kawai T, Rizzo V, et al. Angiotensin II Signal Transduction: An Update on Mechanisms of Physiology and Pathophysiology. *Physiol Rev.* 2018 Jul 1;98(3):1627–738.
3. Rincon-Choles H. ACE inhibitor and ARB therapy: Practical recommendations. *Cleve Clin J Med.* 2019 Sep 1;86(9):608–11.
4. Gekle M, Dubourg V, Schwerdt G, Benndorf RA, Schreier B. The role of EGFR in vascular AT1R signaling: From cellular mechanisms to systemic relevance. *Biochem Pharmacol.* 2023;217:115837.
5. Sparks MA, Crowley SD, Gurley SB, Mirotsoy M, Coffman TM. Classical Renin-Angiotensin System in Kidney Physiology. *Compr Physiol.* 2014 Jul;4(3):1201–28.
6. Khurana V, Goswami B. Angiotensin converting enzyme (ACE). *Clin Chim Acta.* 2022 Jan 1;524:113–22.
7. Thomas WG, Mendelsohn FAO. Angiotensin receptors: form and function and distribution. *Int J Biochem Cell Biol.* 2003 Jun 1;35(6):774–9.
8. Bader M, Steckelings UM, Alenina N, Santos RAS, Ferrario CM. Alternative Renin-Angiotensin System. *Hypertension.* 2024 May;81(5):964–76.
9. Yugandhar VG, Clark MA. Angiotensin III: a physiological relevant peptide of the renin angiotensin system. *Peptides.* 2013;46:26–32.
10. Goodfriend TL. Aldosterone—A Hormone of Cardiovascular Adaptation and Maladaptation. *J Clin Hypertens.* 2007 Jan 31;8(2):133–9.
11. Fitzsimons JT. Angiotensin, Thirst, and Sodium Appetite. *Physiol Rev.* 1998 07;78(3):583–686.
12. Sandgren JA, Linggongoro DW, Zhang SY, Sapouckey SA, Claflin KE, Pearson NA, et al. Angiotensin AT1A receptors expressed in vasopressin-producing cells of the supraoptic nucleus contribute to osmotic control of vasopressin. *Am J Physiol - Regul Integr Comp Physiol.* 2018 Jun 1;314(6):R770–80.
13. Ichikawa I, Harris RC. Angiotensin actions in the kidney: Renewed insight into the old hormone. *Kidney Int.* 1991 Oct 1;40(4):583–96.
14. Chai SY, Fernando R, Peck G, Ye SY, Mendelsohn FAO, Jenkins TA, et al. What's new in the renin-angiotensin system? *Cell Mol Life Sci CMLS.* 2004 Nov 1;61(21):2728–37.
15. Hrenak J, Paulis L, Simko F. Angiotensin A/Alamandine/MrgD Axis: Another Clue to Understanding Cardiovascular Pathophysiology. *Int J Mol Sci.* 2016 Jul 20;17(7):1098.

16. Beyerstedt S, Casaro EB, Rangel ÉB. COVID-19: angiotensin-converting enzyme 2 (ACE2) expression and tissue susceptibility to SARS-CoV-2 infection. *Eur J Clin Microbiol Infect Dis*. 2021 May 1;40(5):905–19.
17. Rao A, Bhat SA, Shibata T, Giani JF, Rader F, Bernstein KE, et al. Diverse biological functions of the renin-angiotensin system. *Med Res Rev*. 2024;44(2):587–605.
18. Tóth AD, Turu G, Hunyady L, Balla A. Novel mechanisms of G-protein-coupled receptors functions: AT1 angiotensin receptor acts as a signaling hub and focal point of receptor cross-talk. *Best Pract Res Clin Endocrinol Metab*. 2018 Apr;32(2):69–82.
19. Rovati GE, Capra V, Neubig RR. The Highly Conserved DRY Motif of Class A G Protein-Coupled Receptors: Beyond the Ground State. *Mol Pharmacol*. 2007 Apr 1;71(4):959–64.
20. Zhang D, Liu Y, Zaidi SA, Xu L, Zhan Y, Chen A, et al. Structural insights into angiotensin receptor signaling modulation by balanced and biased agonists. *EMBO J*. 2023 Jun 1;42(11):e112940.
21. Trzaskowski B, Latek D, Yuan S, Ghoshdastider U, Debinski A, Filipek S. Action of Molecular Switches in GPCRs - Theoretical and Experimental Studies. *Curr Med Chem*. 2012 Mar;19(8):1090–109.
22. Unal H, Jagannathan R, Bhat MB, Karnik SS. Ligand-specific Conformation of Extracellular Loop-2 in the Angiotensin II Type 1 Receptor. *J Biol Chem*. 2010 May 21;285(21):16341–50.
23. Zhang H, Unal H, Gati C, Han GW, Liu W, Zatsepin NA, et al. Structure of the Angiotensin Receptor Revealed by Serial Femtosecond Crystallography. *Cell*. 2015 May 7;161(4):833–44.
24. Hall S, Ward ND, Patel R, Amin-Javaheri A, Lanford H, Grespin RT, et al. Mechanical activation of the angiotensin II type 1 receptor contributes to abdominal aortic aneurysm formation. *JVS-Vasc Sci*. 2021 Jan 1;2:194–206.
25. Gironacci MM, Bruna-Haupt E. Unraveling the crosstalk between renin-angiotensin system receptors. *Acta Physiol*. 2024;240(5):e14134.
26. Hunyady L, Catt KJ. Pleiotropic AT1 receptor signaling pathways mediating physiological and pathogenic actions of angiotensin II. *Mol Endocrinol Baltim Md*. 2006 May;20(5):953–70.
27. Hilger D, Masureel M, Kobilka BK. Structure and dynamics of GPCR signaling complexes. *Nat Struct Mol Biol*. 2018 Jan;25(1):4–12.
28. Tian Y, Smith RD, Balla T, Catt KJ. Angiotensin II Activates Mitogen-Activated Protein Kinase Via Protein Kinase C and Ras/Raf-1 Kinase in Bovine Adrenal Glomerulosa Cells. *Endocrinology*. 1998 Apr 1;139(4):1801–9.
29. Liao DF, Duff JL, Daum G, Pelech SL, Berk BC. Angiotensin II Stimulates MAP Kinase Kinase Kinase Activity in Vascular Smooth Muscle Cells. *Circ Res*. 1996 Nov;79(5):1007–14.

30. Tan M, Xu X, Ohba M, Cui MZ. Angiotensin II–Induced Protein Kinase D Activation Is Regulated by Protein Kinase C δ and Mediated via the Angiotensin II Type 1 Receptor in Vascular Smooth Muscle Cells. *Arterioscler Thromb Vasc Biol.* 2004 Dec;24(12):2271–6.
31. Kelly DJ, Cox AJ, Gow RM, Zhang Y, Kemp BE, Gilbert RE. Platelet-Derived Growth Factor Receptor Transactivation Mediates the Trophic Effects of Angiotensin II In Vivo. *Hypertension.* 2004 01;44(2):195–202.
32. Griendling KK, Ushio-Fukai M. Reactive oxygen species as mediators of angiotensin II signaling. *Regul Pept.* 2000 Jul 28;91(1):21–7.
33. Griendling KK, Minieri CA, Ollerenshaw JD, Alexander RW. Angiotensin II stimulates NADH and NADPH oxidase activity in cultured vascular smooth muscle cells. *Circ Res.* 1994 Jun;74(6):1141–8.
34. Queiroz TM, Monteiro MM, Braga VA. Angiotensin-II-derived reactive oxygen species on baroreflex sensitivity during hypertension: new perspectives. *Front Physiol* [Internet]. 2013 May 13 [cited 2025 Aug 29];4. Available from: <https://www.frontiersin.org/journals/physiology/articles/10.3389/fphys.2013.00105/full>
35. Xi XP, Graf K, Goetze S, Fleck E, Hsueh WA, Law RE. Central role of the MAPK pathway in ang II-mediated DNA synthesis and migration in rat vascular smooth muscle cells. *Arterioscler Thromb Vasc Biol.* 1999;19(1):73–82.
36. Zhang W, Liu HT. MAPK signal pathways in the regulation of cell proliferation in mammalian cells. *Cell Res.* 2002 Mar;12(1):9–18.
37. González-Rubio G, Sellers-Moya Á, Martín H, Molina M. A walk-through MAPK structure and functionality with the 30-year-old yeast MAPK Slt2. *Int Microbiol.* 2021 Nov 1;24(4):531–43.
38. Huang CY, Tan TH. DUSPs, to MAP kinases and beyond. *Cell Biosci.* 2012 Jul 9;2(1):24.
39. Mehta PK, Griendling KK. Angiotensin II cell signaling: physiological and pathological effects in the cardiovascular system. *Am J Physiol Cell Physiol.* 2007 Jan;292(1):C82-97.
40. Keyes J, Ganesan A, Molinar-Inglis O, Hamidzadeh A, Zhang J, Ling M, et al. Signaling diversity enabled by Rap1-regulated plasma membrane ERK with distinct temporal dynamics. *eLife.* 9:e57410.
41. Liu R, Molkentin JD. Regulation of cardiac hypertrophy and remodeling through the dual-specificity MAPK phosphatases (DUSPs). *J Mol Cell Cardiol.* 2016;101:44–9.
42. Owens DM, Keyse SM. Differential regulation of MAP kinase signalling by dual-specificity protein phosphatases. *Oncogene.* 2007 May 14;26(22):3203–13.
43. Chen HF, Chuang HC, Tan TH. Regulation of Dual-Specificity Phosphatase (DUSP) Ubiquitination and Protein Stability. *Int J Mol Sci.* 2019 May 30;20(11):2668.
44. Gumpena R, Lountos GT, Raran-Kurussi S, Tropea JE, Cherry S, Waugh DS. Crystal structure of the human dual specificity phosphatase 1 catalytic domain. *Protein Sci Publ Protein Soc.* 2018 Feb;27(2):561–7.

45. Seternes OM, Kidger AM, Keyse SM. Dual-specificity MAP kinase phosphatases in health and disease. *Biochim Biophys Acta Mol Cell Res.* 2019 Jan;1866(1):124–43.
46. Voldborg BR, Damstrup L, Spang-Thomsen M, Poulsen HS. Epidermal growth factor receptor (EGFR) and EGFR mutations, function and possible role in clinical trials. *Ann Oncol Off J Eur Soc Med Oncol.* 1997;8(12):1197–206.
47. Levantini E, Maroni G, Del Re M, Tenen DG. EGFR signaling pathway as therapeutic target in human cancers. *Semin Cancer Biol.* 2022 Oct;85:253–75.
48. King LE, Gates RE, Stoscheck CM, Nanney LB. Epidermal growth factor/transforming growth factor alpha receptors and psoriasis. *J Invest Dermatol.* 1990;95(5 Suppl):10S-12S.
49. Liu Y, Li P, Jiang T, Li Y, Wang Y, Cheng Z. Epidermal growth factor receptor in asthma: A promising therapeutic target? *Respir Med.* 2023 Feb;207:107117.
50. Sigismund S, Avanzato D, Lanzetti L. Emerging functions of the EGFR in cancer. *Mol Oncol.* 2018;12(1):3–20.
51. Cao S, Pan Y, Terker AS, Arroyo Ornelas JP, Wang Y, Tang J, et al. Epidermal growth factor receptor activation is essential for kidney fibrosis development. *Nat Commun.* 2023 Nov 14;14(1):7357.
52. Lurje G, Lenz HJ. EGFR Signaling and Drug Discovery. *Oncology.* 2010 Feb 2;77(6):400–10.
53. Rath N, Wang Z, Lu MM, Morrisey EE. LMCD1/Dyxin Is a Novel Transcriptional Cofactor That Restricts GATA6 Function by Inhibiting DNA Binding. *Mol Cell Biol.* 2005 Oct;25(20):8864–73.
54. Whitcomb J, Gharibeh L, Nemer M. From embryogenesis to adulthood: Critical role for GATA factors in heart development and function. *IUBMB Life.* 2020;72(1):53–67.
55. Ye Z, Chen G, Hou C, Jiang Z, Wang E, Wang J. LMCD1 facilitates the induction of pluripotency via cell proliferation, metabolism, and epithelial-mesenchymal transition. *Cell Biol Int.* 2022 Sep;46(9):1409–22.
56. Frank D, Frauen R, Hanselmann C, Kuhn C, Will R, Gantenberg J, et al. Lmcd1/Dyxin, a novel Z-disc associated LIM protein, mediates cardiac hypertrophy in vitro and in vivo. *J Mol Cell Cardiol.* 2010 Oct;49(4):673–82.
57. Janjanam J, Zhang B, Mani AM, Singh NK, Traylor JG, Orr AW, et al. LIM and cysteine-rich domains 1 is required for thrombin-induced smooth muscle cell proliferation and promotes atherogenesis. *J Biol Chem.* 2018 Mar 2;293(9):3088–103.
58. Govatati S, Pichavaram P, Janjanam J, Guo L, Virmani R, Rao GN. Myristoylation of LMCD1 leads to its species-specific derepression of E2F1 and NFATc1 in the modulation of CDC6 and IL-33 expression during development of vascular lesions. *Arterioscler Thromb Vasc Biol.* 2020 May;40(5):1256–74.
59. Pacurari M, Kafoury R, Tchounwou PB, Ndebele K. The Renin-Angiotensin-aldosterone system in vascular inflammation and remodeling. *Int J Inflamm.* 2014;2014:689360.

60. Te Riet L, van Esch JHM, Roks AJM, van den Meiracker AH, Danser AHJ. Hypertension: renin-angiotensin-aldosterone system alterations. *Circ Res*. 2015 Mar 13;116(6):960–75.
61. Bogatkevich GS, Atanelishvili I, Bogatkevich AM, Silver RM. Increased Expression of LMCD1 in Scleroderma-Associated Interstitial Lung Disease is Critical for Profibrotic Characteristics of Lung Myofibroblasts. *Arthritis Rheumatol Hoboken NJ*. 2023 Mar;75(3):438–48.
62. Ferreira DMS, Cheng AJ, Agudelo LZ, Cervenka I, Chaillou T, Correia JC, et al. LIM and cysteine-rich domains 1 (LMCD1) regulates skeletal muscle hypertrophy, calcium handling, and force. *Skelet Muscle*. 2019 Oct 31;9(1):26.
63. Eguchi S, Dempsey PJ, Frank GD, Motley ED, Inagami T. Activation of MAPKs by angiotensin II in vascular smooth muscle cells. Metalloprotease-dependent EGF receptor activation is required for activation of ERK and p38 MAPK but not for JNK. *J Biol Chem*. 2001 Mar 16;276(11):7957–62.
64. Ebrahimian T, Li MW, Lemarié CA, Simeone SMC, Pagano PJ, Gaestel M, et al. Mitogen-Activated Protein Kinase–Activated Protein Kinase 2 in Angiotensin II–Induced Inflammation and Hypertension. *Hypertension*. 2011 Feb;57(2):245–54.
65. Kovács KB, Szalai L, Szabó P, Gém JB, Barsi S, Szalai B, et al. An Unexpected Enzyme in Vascular Smooth Muscle Cells: Angiotensin II Upregulates Cholesterol-25-Hydroxylase Gene Expression. *Int J Mol Sci*. 2023 Jan;24(4):3968.
66. Clerk A, Sugden PH. Inflammation My Heart (by p38-MAPK). *Circ Res*. 2006 Sep;99(5):455–8.
67. Wang J, Liu Y, Guo Y, Liu C, Yang Y, Fan X, et al. Function and inhibition of P38 MAP kinase signaling: Targeting multiple inflammation diseases. *Biochem Pharmacol*. 2024 Feb 1;220:115973.
68. Touyz RM, Wu XH, He G, Salomon S, Schiffrin EL. Increased angiotensin II-mediated Src signaling via epidermal growth factor receptor transactivation is associated with decreased C-terminal Src kinase activity in vascular smooth muscle cells from spontaneously hypertensive rats. *Hypertens Dallas Tex 1979*. 2002 Feb;39(2 Pt 2):479–85.
69. Min LJ, Mogi M, Iwai M, Horiuchi M. Signaling mechanisms of angiotensin II in regulating vascular senescence. *Ageing Res Rev*. 2009 Apr 1;8(2):113–21.
70. Caunt CJ, Keyse SM. Dual-specificity MAP kinase phosphatases (MKPs). *Febs J*. 2013 Jan;280(2):489–504.
71. Patterson KI, Brummer T, O'Brien PM, Daly RJ. Dual-specificity phosphatases: critical regulators with diverse cellular targets. *Biochem J*. 2009 Mar 15;418(3):475–89.
72. Lindauer M, Hochhaus A. Dasatinib. *Recent Results Cancer Res Fortschritte Krebsforsch Progres Dans Rech Sur Cancer*. 2018;212:29–68.
73. Iqbal N, Iqbal N. Imatinib: A Breakthrough of Targeted Therapy in Cancer. *Chemother Res Pract*. 2014 May 19;2014:357027.

9. Bibliography of candidate's publications

9.1. Publications relevant to the dissertation

- I. **Gém, Janka Borbála** ; Kovács, Kinga Bernadett ; Szalai, Laura ; Szakadáti, Gyöngyi ; Porkoláb, Edit ; Szalai, Bence ; Turu, Gábor ; Tóth, András Dávid ; Szekeres, Mária ; Hunyady, László ; Balla, András. Characterization of Type 1 Angiotensin II Receptor Activation Induced Dual-Specificity MAPK Phosphatase Gene Expression Changes in Rat Vascular Smooth Muscle Cells , Cells, 2021 Dec 15;10(12):3538. **IF(2021): 7.666**
- II. **Gém, Janka Borbála**; Kovács, Kinga Bernadett; Barsi, Szilvia; Hadadnejadtehrani, Saba; Damouni, Amir; Turu, Gábor; Tóth, András Dávid; Várnai, Péter; Hunyady, László; Balla, András. Role of LMCD1 in the Long-Term Effects of Angiotensin II in Vascular Smooth Muscle Cells, International Journal of Molecular Sciences, 2025 Apr 25;26(9):4053, **IF(2024): 4,9**

Cumulative impact factor: 12,566

9.2. Publications unrelated to the dissertation

- I. Kovács, Kinga Bernadett ; Szalai, Laura ; Szabó, Pál ; **Gém, Janka Borbála** ; Barsi, Szilvia ; Szalai, Bence ; Perey-Simon, Bernadett ; Turu, Gábor ; Tóth, András Dávid ; Várnai, Péter ; Hunyady, László ; Balla, András. An Unexpected Enzyme in Vascular Smooth Muscle Cells: Angiotensin II Upregulates Cholesterol-25-Hydroxylase Gene Expression ; International Journal of Molecular Sciences, 2023 Feb 16;24(4):3968.. **IF(2023): 4,9**
- II. Vass, Zsolt; Shenker-Horváth, Kinga; Bányai, Bálint; Vető, Kinga Nóra, Török, Viktória; **Gém, Janka Borbála**; Nádasy, György L; Kovács, Kinga Bernadett; Horváth, Eszter Mária; Jakus, Zoltán; Hunyady, László; Szekeres, Mária; Dörnyei, Gabriella. Investigating the Role of Cannaboid Type 1 Receptors in Vascular Function and Remodeling in Hypercholesterolemic Mouse Model with Low-Density Lipoprotein-Cannaboid Type 1 Receptor Double Knockout Animals. International Journal of Molecular Sciences, 2024 Sep 2;25(17):9537. **IF(2024): 4,9**

Cumulative impact factor of all publications: 22,366

Cumulative impact factor of first author and shared first author publications: 12,566

10. Acknowledgements

I would like to express my sincere gratitude to Dr. András Balla and Prof. Dr. László Hunyady, who guided and supported my research work throughout this journey as my tutors. Their expert guidance and encouragement were invaluable to the completion of my dissertation. I am also grateful to Prof. Dr. Attila Mócsai, the director of the Department of Physiology, and Prof. Dr. Péter Várnai, the head of the Molecular Medicine Division, for their significant support and assistance. I would like to extend my heartfelt thanks to all my colleagues at the Molecular Endocrinology Laboratory and Cell Signaling Laboratory, furthermore to all my colleagues from the Department of Physiology, whose help and collaboration were essential to my PhD work. I would also like to say thank you for all my friends and family, who stood beside me and supported me during my PhD years. Thank you!